ELSEVIER

Palaeogeography, Palaeoclimatology, Palaeoecology 191 (2003) 65–109

PALAEO

www.elsevier.com/locate/palaeo

Carnian–Norian biomagnetostratigraphy at Silická Brezová (Slovakia): correlation to other Tethyan sections and to the Newark Basin

J.E.T. Channell [a,*], H.W. Kozur [b], T. Sievers [a], R. Mock [c,1], R. Aubrecht [c], M. Sykora [c]

[a] *Department of Geological Sciences, University of Florida, Gainesville, FL 32611-2120, USA*
[b] *Rézsü u. 83, H 1029, Budapest, Hungary*
[c] *Department of Geology and Paleontology, Comenius University, 84215 Bratislava, Slovak Republic*

Received 23 April 2002; received in revised form 11 November 2002; accepted 25 November 2002

Abstract

Correlations of Upper Triassic magnetic stratigraphies from Tethyan sections have been hampered by difficulties with conodont biostratigraphy and taxonomy, and discontinuous sedimentation, particularly in the 'Hallstatt Limestones' of Turkey and Austria. The magnetic stratigraphy and conodont biostratigraphy from the Upper Carnian to Upper Norian limestones exposed at Silická Brezová (Slovakia) can be correlated to other Tethyan sections and to the continental succession in the Newark Basin. The resulting correlations help to resolve some of the apparent discrepancies in existing conodont zonations, and result in a revised correlation to North American terrestrial vertebrate and palynological zones. The correlations imply that the Norian–Rhaetian boundary lies within Newark polarity zone E17r at ~207 Ma. The Carnian–Norian boundary lies close to the base of Newark polarity zone E7r at ~226 Ma. This implies durations for the Norian and Rhaetian stages of 19 Myr and 7 Myr, respectively.

Keywords: Upper Triassic; conodont biostratigraphy; magnetostratigraphy; marine/terrestrial correlations

1. Introduction

Magnetic polarity stratigraphy has proved to be particularly useful for correlating sedimentary sequences from contrasting environments with diverse biostratigraphies. For example, magnetic stratigraphy has been the basis for the correlation of Cenozoic North American land mammal ages to geologic stage boundaries defined on the basis of marine fossils (see Opdyke and Channell, 1996). Between 1990 and 1993 the Newark Basin Coring Project produced a more or less complete drill-core record of the ~5 km lacustrine section of Late Carnian (Late Triassic) to Hettangian (Early Jurassic) age. The recovered sedimentary

[1] Deceased.

* Corresponding author. Fax: +1-352-392-9294.
E-mail address: jetc@ufl.edu (J.E.T. Channell).

0031-0182/02/$ – see front matter © 2002 Elsevier Science B.V. All rights reserved.
doi:10.1016/S0031-0182(02)006545

section yielded a well-defined magnetic stratigraphy featuring 59 polarity zones (Kent et al., 1995; Olsen and Kent, 1996, 1999; Kent and Olsen, 1999, 2000). Lithologic facies response to climatically induced lake level variation, determined by depth sensitive sedimentary structures and sediment color, yielded a full spectrum of Milankovitch cyclicity (Olsen and Kent, 1996, 1999; Kent and Olsen, 1999, 2000). By assuming that the dominant (McLaughlin) lake level cycles represent 404 kyr orbital eccentricity cycles, and by anchoring the timescale by adopting an age of 202 Ma for the Triassic–Jurassic boundary, Kent and Olsen (1999) generated a calibrated polarity timescale for the 30 Myr Newark Basin record.

The objective of this paper is to obtain a magnetic stratigraphy from a marine conodont-bearing section coeval with the Newark Basin in order to correlate a marine conodont biostratigraphy to the Newark Basin astrochronology. We chose a 140-m-thick section of Late Carnian to latest Norian age exposed at Silická Brezová (Slovakia). The stratigraphy comprises predominantly red to gray pelagic limestones (Hallstatt Limestone facies) with crinoid–brachiopod limestone in the lower part. The term 'Hallstatt Limestones' was coined in the Alps and West Carpathian Mountains and refers to the Middle and Upper Triassic, mostly reddish and gray pelagic limestones deposited at the outer shelf and slope of the Meliata–Hallstatt Ocean under conditions of low terrigenous input. The name derives from the typical development of this facies around Hallstatt in the region of Salzburg (Austria). The Hallstatt Limestones are a time-transgressive Scythian to Upper Triassic pelagic gray to red, commonly condensed, sometimes nodular limestone facies widely distributed from Austria to Timor (Southeast Asia). Over this long distance, the facies succession within the Hallstatt Limestone facies is similar. The succession at Silická Brezová is expanded relative to most Hallstatt Limestone sections, and initial conodont studies indicated a complete record of Upper Carnian (Tuvalian) to Upper Norian (Sevatian) conodont zones (Kozur and Mock, 1972a,b, 1973a,b, 1974a,d; Kozur, 1972; Mock, 1980). The conodont alteration index (CAI) is 2, implying maximum temperatures of 60° to 140°C since deposition (Nowlan and Barnes, 1987).

Existing marine Upper Triassic magnetic stratigraphies have been derived from various pelagic limestone facies, from extremely condensed Hallstatt Limestones to rapidly deposited calciturbidites. Sections have been studied in Turkey, at Bolücektası Tepe (Gallet et al., 1992), at Kavur Tepe (Gallet et al., 1993), at Erenkolu Mezarlik (Gallet et al., 1994) and at Kavaalani (Gallet et al., 2000). In Austria, sections have been studied at Mayerling (Gallet et al., 1994) and at Scheiblkogel (Gallet et al., 1996). Bio–magnetostratigraphic correlations from one section to another, and to Newark, have remained equivocal. The problem may lie with extremely variable sedimentation rates, hiatuses, lack of thick continuous sections, and poor resolution of conodonts in rocks unsuitable for conodont biostratigraphy. For instance, the Erenkolu Mezarlik section consists of ~5 m of extremely condensed Hallstatt Limestone for the interval from the base of the Carnian up to the Lower Norian. The Kavur Tepe section consists of 30 m of Norian Hallstatt Limestones representing seven conodont zones from the middle part of the Lower Norian (lower *Epigondolella triangularis–Norigondolella hallstattensis* Zone) up to the lower part of Upper Sevatian *Misikella hernsteini–Parvigondolella andrusovi* Zone. The overlying rapidly accumulated calciturbidites yield only a few conodonts tentatively assigned to the Late Sevatian (and Rhaetian). The Bolücektası Tepe section begins with about 9 m of condensed Upper Ladinian to Lower Carnian nodular Hallstatt Limestones, followed by a hiatus, and then uppermost Carnian to Lower Norian beds (about 10 m of light-colored bedded limestones and 24 m of massive to thick-bedded, strongly faulted, light-colored pelagic limestones). The section ends with more than 35 m of whitish, subordinately pinkish, calciturbidites of Middle Norian age.

Muttoni et al. (2001) sampled a more expanded facies, nodular *Halobia*-bearing cherty calcilutites, spanning the Carnian–Norian boundary in Sicily at Pizzo Mondello. Here the sedimentation rates are mainly in the 13–46 m/Myr range, but again the correlation to Newark is equivocal, as there is no clear 'fingerprint' in the polarity zone pattern.

2. Geological background and sampling

The sampled Carnian–Norian (Upper Triassic) outcrops at Silická Brezová are located ~1 km west of the village of the same name (Fig. 1). This region of South Slovakia, close to the Hungarian border, is referred to as the Slovak Karst. The tectonic unit that occupies most of this region is the Silica Nappe (Kozur and Mock, 1973a,c) which is the uppermost tectonic unit of the Inner West Carpathians and comprises Upper Permian to Middle Jurassic strata (see Kozur and Mock, 1997). The Middle and Upper Triassic limestones of the Silica Nappe were deposited on the passive continental margin to the north of the Meliata Ocean, which opened in the West Carpathians

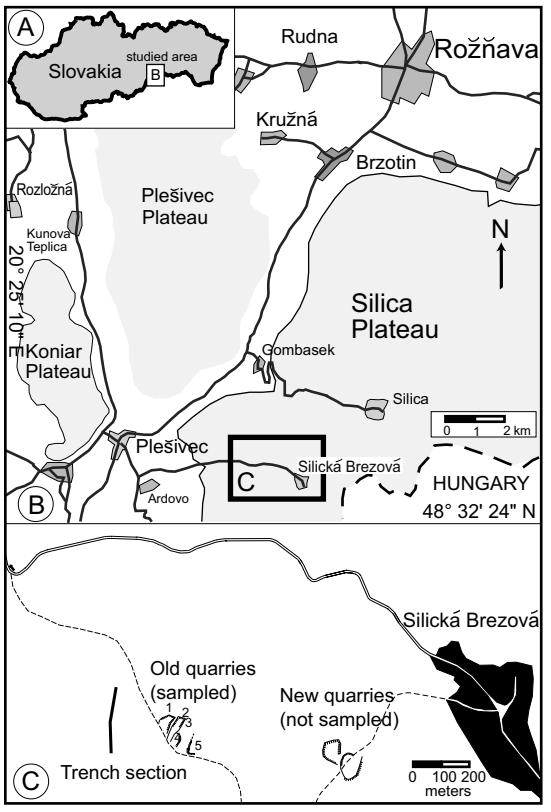

Fig. 1. Location of the Silická Brezová sections. (A) Investigated area relative to the outline of Slovakia. (B) Investigated area within the Silica Plateau. (C) Investigated sections west of Silická Brezová. Key: (1) West Quarry; (2) Frontal Quarry; (3) Right Quarry; (4) Lower Quarry; (5) Massiger Hellkalk Quarry.

during the Late Bithynian (latest Early Anisian). Sea-floor spreading in the Meliata Ocean was short-lived and ceased in the Middle Carnian (Kozur, 1991). Accelerated thermal subsidence following cessation of spreading is marked in the stratigraphy of the Silica Nappe by a facies change from Middle Carnian white shallow-water algal (Wetterstein) limestones through light-gray, partly pinkish crinoid–brachiopod limestone, to Upper Carnian white to red pelagic (Hallstatt) Limestones. Compressional tectonics affected the Meliata Ocean from Rhaetian (latest Triassic) time, with Jurassic subduction culminating in Late Jurassic (Middle Oxfordian) collision of the two facing continental margins. During the collision, the Silica Nappe was thrust toward the south over the oceanic accretionary complex of the Meliaticum. Subduction of the Meliata Ocean was coeval with the opening of the Penninic (Magura and Pieniny) oceans to the north (see Kozur and Mock, 1996, 1997; Channell and Kozur, 1997). Southward-dipping subduction of the Penninic oceans led to the northward thrusting of the Silica Nappe and northward-rooted nappes during the Late Cretaceous and Cenozoic to form the present architecture of the West Carpathian Mountains.

The microfauna (conodonts, holothurian sclerites, ostracods, radiolarians) and dasycladacean flora of the Middle and Upper Triassic limestones at Silická Brezová were described by Bystrický (1964), Kozur (1972, 1998), Kozur and Mock (1972a,b, 1973a,b, 1974a–d), Kozur and Mostler (1972), and Mišík and Borza (1976). The early studies indicated an apparently complete conodont zonation from Upper Carnian (somewhat above the Julian–Tuvalian boundary) to uppermost Norian in about 140 m of stratigraphic section partially exposed on a hillside about 1.3 km west of the village of Silická Brezová (Fig. 1). The Lower Norian part of the section is well exposed in a series of quarries located 200 m to the east of the main section. As part of this project, one of us (R.M.) arranged for the main section to be excavated by a group of professional ditch-diggers. The excavation resulted in the complete exposure of a 140-m section, and indicated the presence of a previously poorly exposed interval of slumping

and brecciation in the upper part of the Lower Norian and Middle Norian parts of the section. Therefore, we divide the paleomagnetically investigated part of the trench section into Lower Trench (below the interval of slumping/brecciation) and Upper Trench (above the interval of slumping/brecciation) (Fig. 2). The slumped/brecciated upper Lower Norian part of the trench section is partly exposed in nearby quarries without slumping or brecciation (Fig. 2). The close

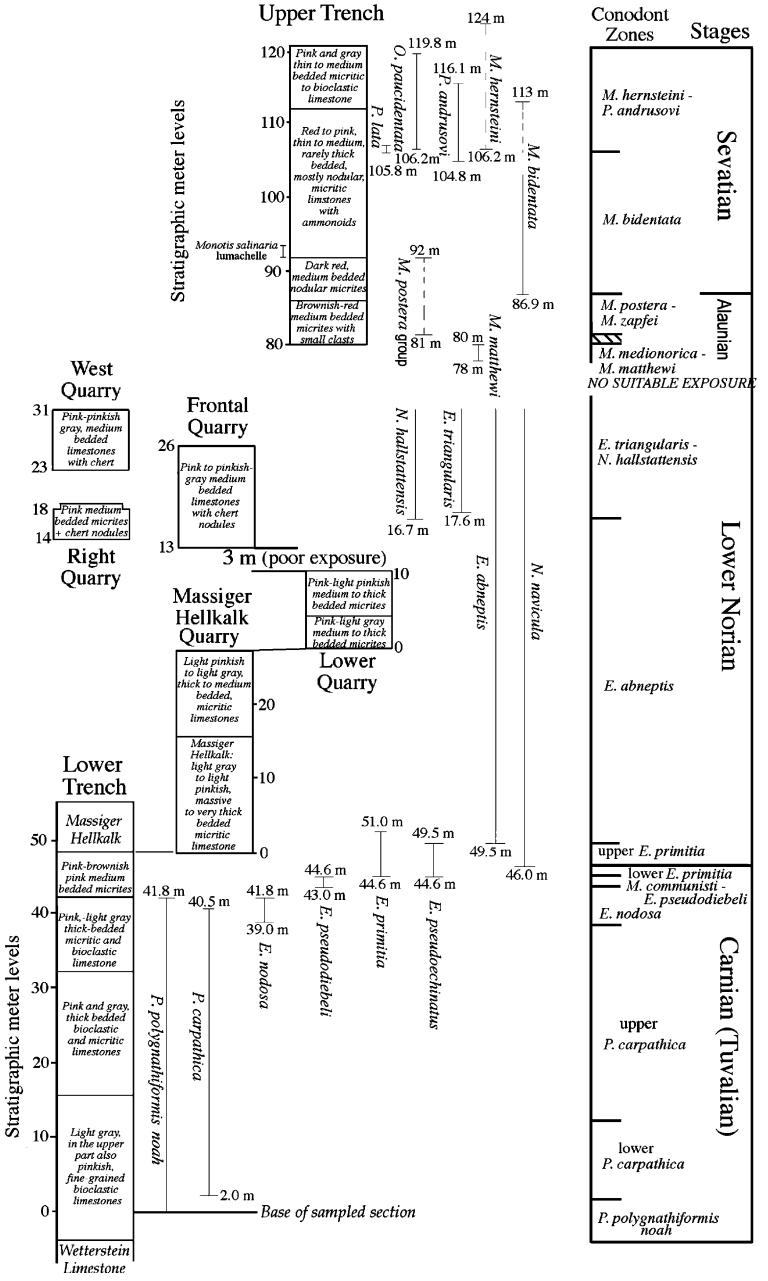

Fig. 2. Schematic representation of the individual stratigraphic sections that comprise the composite section at Silická Brezová. Ranges of index conodonts are indicated.

proximity of contrasting Norian exposures indicates abrupt facies variations on the outer continental shelf and slope.

The upper boundary of the Lower Trench section can be correlated to the 'Massiger Hellkalk Quarry' (Fig. 2) by recognition of the facies change at the base of the Massiger Hellkalk (light-colored massive limestone) unit and by conodonts. Each sampled quarry section can be correlated directly by tracing individual beds with the exception of the link between the Lower Quarry and the Frontal Quarry (Fig. 2). Here the link cannot be walked-out due to poor exposure. We estimate a 3-m stratigraphic interval (without facies change and within one conodont zone) between the top of the Lower Quarry and the base of the Frontal Quarry. Blocks ('float') exposed in the forest floor were sampled to accommodate this gap. The top of the quarry section (top of West Quarry) lies stratigraphically within the upper part of the *Epigondolella triangularis* Zone corresponding to the lower part of the slumped/brecciated interval in the trench section, below the base of Upper Trench (Fig. 2). The uppermost Lower Norian and most of the Middle Norian were therefore not investigated paleomagnetically in the Silická Brezová sections.

About 800 oriented cylindrical (2.5-cm diameter) paleomagnetic samples were collected with a hand-held gasoline-powered drill at decimeter (~25-cm) spacing both in the 140-m trench section and in the ~50 m of stratigraphic section exposed in the quarries. Hand samples for conodont studies were collected initially at about 1-m intervals. Subsequently, the sample spacing was reduced to 10–20 cm in critical parts of the section, such as at conodont zonal boundaries. In addition to the stratigraphic sections illustrated in Fig. 2, paleomagnetic samples were collected from a quarry (referred to as the Fold Test Quarry) located along strike from the Right Quarry. Here the bedding dip is to the south, different from the other quarry sections that dip uniformly to the NNW (at about 30°). The Fold Test Quarry is important for generating a fold test to constrain the age of magnetization components. Samples were also collected from ten clasts in the brecciated interval of the trench section. The number of sampled clasts is limited by the availability of clasts large enough to produce more than one sample per clast. The initial sampling in the quarries was carried out in 1992 and was restricted to the Lower Quarry and Frontal Quarry (Fig. 2). The trench was excavated in 1996. Sampling of the trench and the quarries was carried out in 1996, 1997, 1998, 1999 and 2000. The sections have been paint-marked so that meter levels in the trench and quarries can be recovered for future studies. Some useful coordinates at Silická Brezová: 'West Quarry': 48°31.953′N, 20°28.169′E; 'Fold Test Quarry': 48°31.935′N, 20°28.184′E; 'Front Quarry': 48°31.961′N, 20°28.212′E; 'Right Quarry': 48°31.952′N, 20°28.227′E; 'Massiger Hellkalk Quarry': 48°31.913′N, 20°28.218′E; 'Lower Quarry'–base (4-m level): 48°31.876′N, 20°28.237′E; base of the Trench section: 48°31.781′N, 20°28.171′E; base of the Hallstatt Limestone in Trench section: 48°31.817′N, 20°28.152′E; core of slump fold in the brecciated part of the Trench section: 48°31.867′N, 20°28.101′E; top of the Trench section (tectonic contact): 48°31.918′N, 20°28.047′E.

3. Magnetic properties

Hallstatt Limestones and other Middle–Upper Triassic pelagic limestones have been the subject of paleomagnetic/magnetostratigraphic studies in sections from Turkey (Gallet et al., 1992, 1993, 2000), Greece (Muttoni et al., 1994, 1997), Albania (Muttoni et al., 1996, 1998), Sicily (Muttoni et al., 2001), and Austria (Gallet et al., 1994, 1996). In Slovakia and North Hungary, the Triassic limestones of the Silica Nappe, including Hallstatt Limestones at Silická Brezová, have been studied by Marton et al. (1988, 1991), Kruczyk et al. (1998), and Tunyi et al. (1999) in order to determine the tectonic rotation of the Silica Nappe. Marton et al. (1988, 1991) concluded that a primary magnetization could be isolated at Silická Brezová whereas Kruczyk et al. (1998) concluded that these limestones were remagnetized in the Tertiary.

The consensus of the studies cited above is that

the Hallstatt Limestone facies can carry a primary (Triassic) magnetization and that magnetite is the most important carrier of natural remanent magnetization (NRM). Pigmentary hematite contributes to laboratory-induced isothermal remanent magnetization (IRM) and anhysteretic remanent magnetization and, on the basis of the maximum blocking temperatures of NRM, is an important contributor to the NRM in the reddened samples, but not in the white/pink samples.

Progressive thermal demagnetization of the NRM of samples from Silická Brezová was carried out at 50°C steps up to 250°C, 25°C steps in the 250–500°C interval, and then smaller (either 10° or 15°C) steps until the magnetization intensity fell below magnetometer noise level (total moment $< 10^{-4}$ Am^2). For a sample subset, susceptibility was measured after each remanence measurement in order to monitor mineralogical changes during the thermal demagnetization procedure. Prior to heating, volume susceptibility values are in the range from -10^{-5} to $+10^{-5}$ SI and generally remain within that range over the entire temperature range. For some samples from the Lower Trench, volume susceptibility values rise to values of $2–3\times10^{-5}$ SI after heating above 500°C, indicating mineralogical change above this temperature, possibly due to the pyrite to magnetite transformation in the gray bioclastic limestones that occur in the Lower Trench.

Acquisition of IRM and thermal demagnetization of a three-axis IRM (see Lowrie, 1990) indicates that magnetite and hematite are important magnetic minerals in the Upper Trench but that magnetite dominates the magnetic mineralogy in the Lower Trench and in the quarry sections

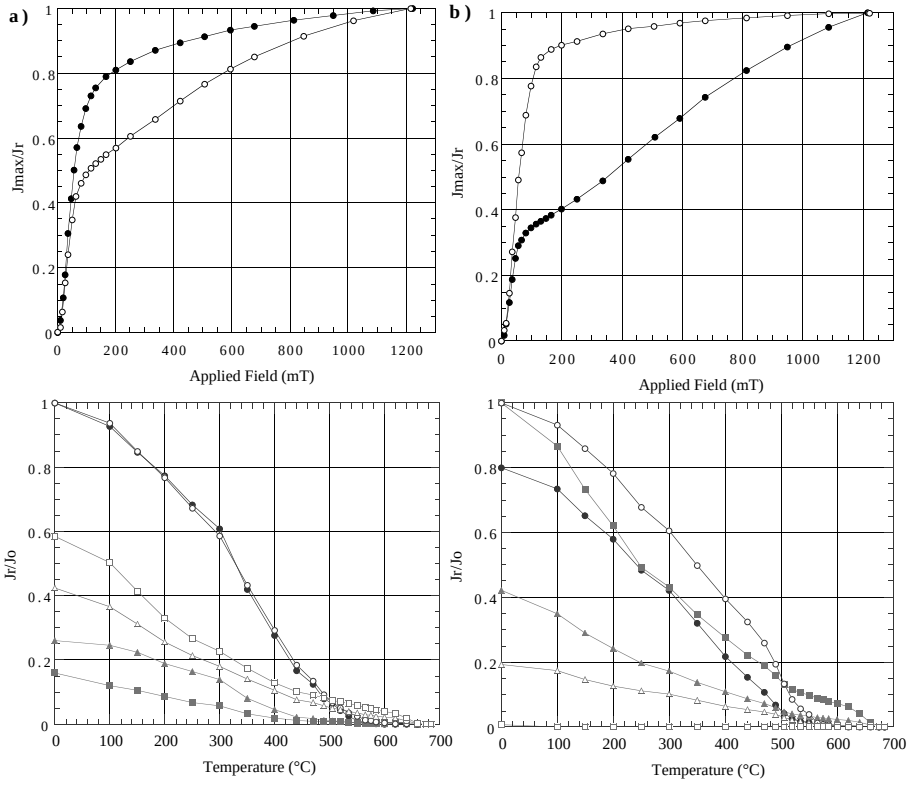

Fig. 3. Top: Acquisition of IRM. Base: Thermal demagnetization of a 3-axis IRM. Circles show soft (120-mT) IRM, triangles show intermediate (400-mT) and squares show hard (1250-mT) IRM. (a) Samples from Lower Trench at 2.00 m (closed symbols) and Frontal Quarry at 22.75 m (open symbols). (b) Samples from Upper Trench at 103.00 m (closed symbols) and Upper Trench at 119.86 m (open symbols).

(Fig. 3). The maximum blocking temperatures of the NRM are below 560°C for the Lower Trench and the quarry sections, and up to ~630°C in the Upper Trench (Fig. 4). We infer from this that magnetite is the principal carrier of NRM in the Lower Trench and the quarry sections, and that hematite contributes to the NRM in Upper Trench. This increased hematite influence is reflected in the increased reddening of the limestones in the Upper Trench (Fig. 2).

Ten clasts in the brecciated interval of the trench (between the Lower Trench and Upper Trench) were sampled in order to determine the age of magnetization components relative to clast emplacement. This constitutes a 'conglomerate test' for the age of magnetization first advocated by Graham (1949). The number of sampled clasts was limited by size of individual clasts, the vast majority being too small to obtain 2.5-cm-diameter cylindrical samples. Orthogonal projection of thermal demagnetization data from clasts (Fig. 5) indicate superimposed magnetization components, with poorer definition of the higher blocking temperature component than usual for the in

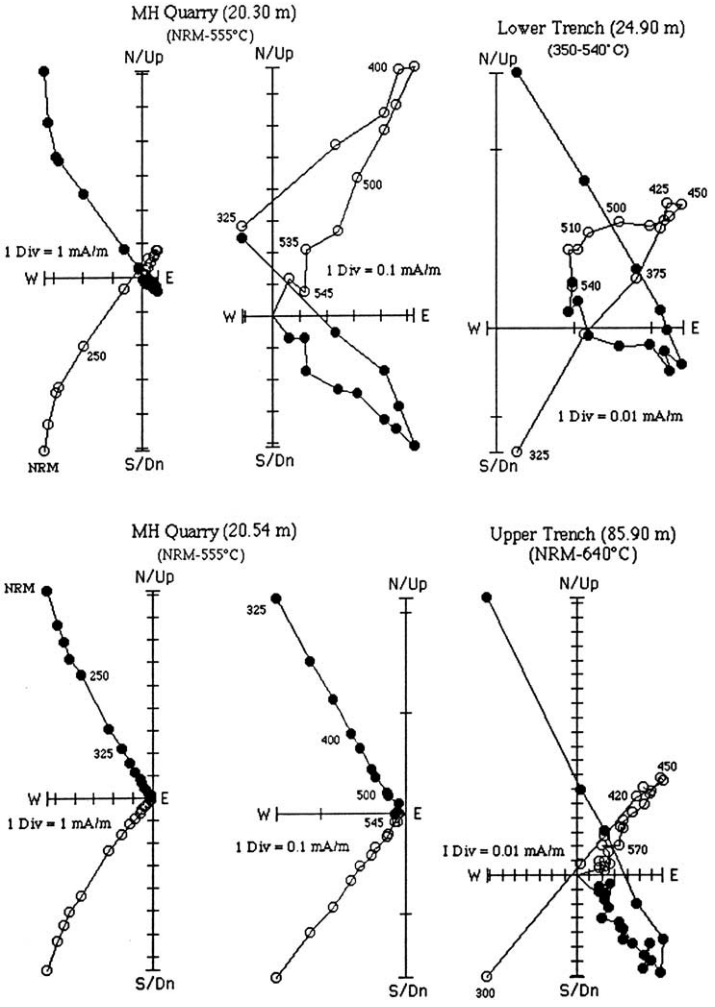

Fig. 4. Orthogonal projection of thermal demagnetization data from the Massiger Hellkalk (MH) Quarry, Lower Trench and Upper Trench. For the MH samples, the projection on the right is a blow-up of the high temperature portion of the projection on the left. Open and closed symbols represent projections of the vector end-point on the vertical and horizontal planes, respectively. Temperatures corresponding to some demagnetization steps are indicated in °C.

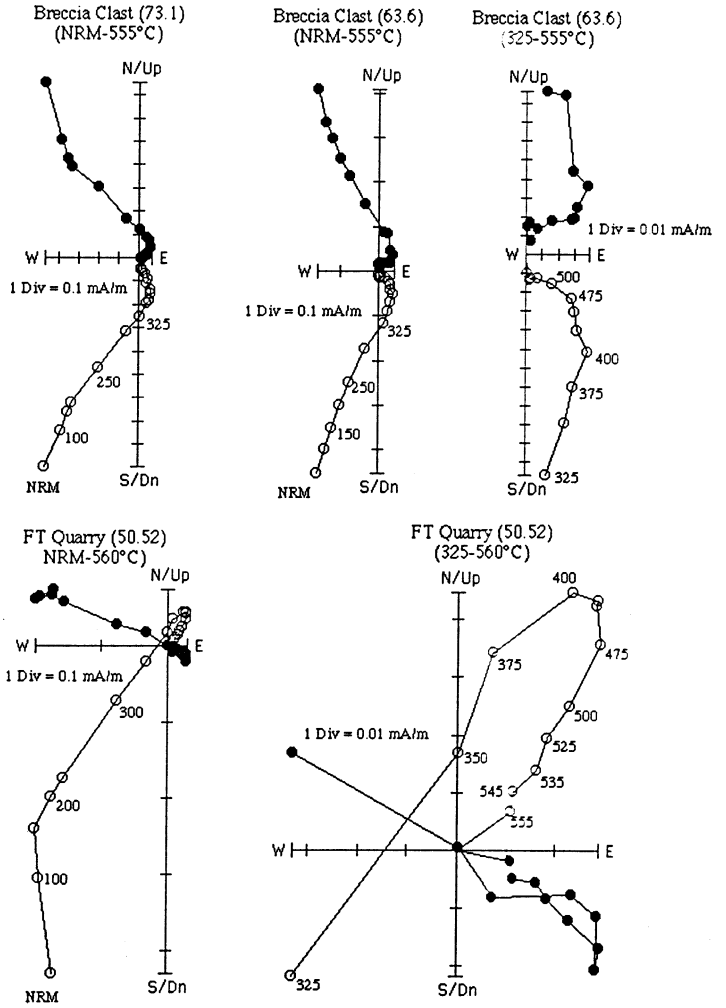

Fig. 5. Orthogonal projection of thermal demagnetization data from breccia clasts (trench section) and from the Fold Test (FT) Quarry. Open and closed symbols represent projections of the vector end-point on the vertical and horizontal planes, respectively. Temperatures corresponding to some demagnetization steps are indicated in °C.

situ sediment. The low blocking temperature (LBT) component is well defined and tightly grouped (Fig. 6a) and the high blocking temperature (HBT) component is dispersed (Fig. 6b) but not random according to the Watson (1956) test for randomness. We conclude that the HBT magnetization component was acquired by the clasts partly prior to and partly after emplacement, and that the LBT component was acquired after emplacement.

For the in situ sediment a normal polarity LBT magnetization component is usually superimposed on a reverse polarity HBT component (Fig. 4). The normal polarity LBT component has a direction that is not distinguishable from the normal polarity HBT component. We resolve the HBT component in the 450–560°C temperature range, and the LBT component in the 200–400°C temperature range using the standard principal component analysis (Kirschvink, 1980). The LBT magnetization direction has normal polarity (Fig. 7a), whereas the HBT component has dual polarity (Fig. 7b). Individual HBT component directions from the Upper Trench are more scat-

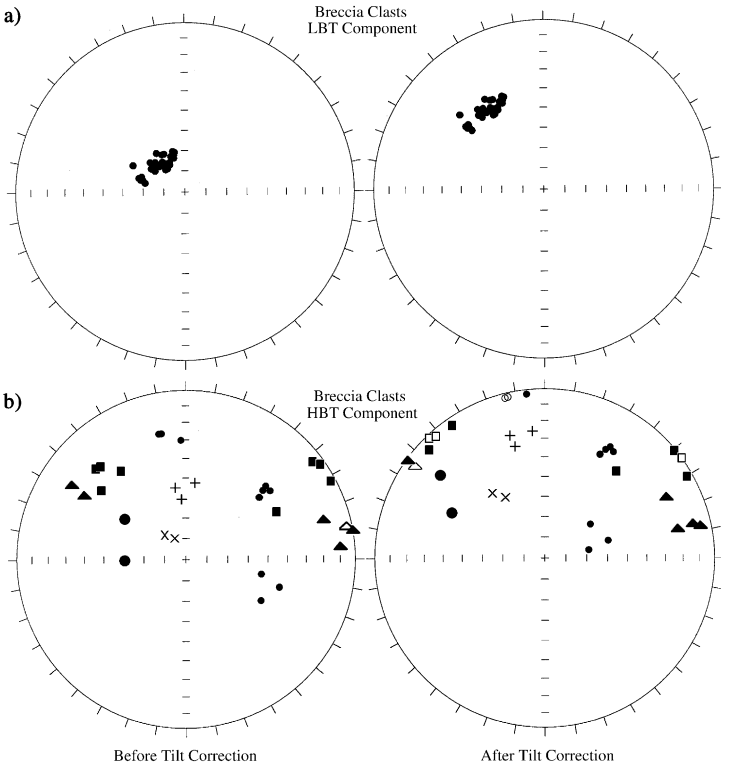

Fig. 6. Equal area projections of LBT components (top) and HBT components (below) from breccia clasts. For the HBT plot, like symbols indicate component directions from the same clast. Data are from ten clasts. Closed symbols and crosses represent downward inclinations. Open symbols represent upward inclinations.

tered relative to those from the Lower Trench (Fig. 7b). The HBT components in the Upper Trench are often difficult to resolve. We attribute this to the increased influence/grain size of hematite in the Upper Trench, which increases the maximum blocking temperature of the LBT, resulting in more overlap of the blocking temperature spectra of the LBT and HBT components.

Apart from the sections depicted in Fig. 2, 45 samples were collected from an additional quarry (Fold Test Quarry) which is located along strike from the Right Quarry. The reason for sampling here was that the bedding dip is 21° to the south in contrast to the NNW dips seen in the other quarry sections, thus facilitating the fold test to determine the ages of magnetization components relative to tectonic tilting. The fold test of McFadden (1990) is indeterminate for the LBT site mean directions from the eight sampled sections (Fig. 7a). For HBT site mean directions, the fold test is positive at the 95% confidence level (Fig. 7b), implying that the HBT components pre-date tectonic tilting. The age of deformation and emplacement of the Silica Nappe spans the Jurassic to Neogene, beginning with the demise of the Meliata Ocean and culminating in the subduction of the Penninic oceans and the subsequent Neogene extension in the Pannonian Basin. Due to the range of deformation ages, the positive fold test does not pinpoint the age of the HBT component but does tell us that the HBT component pre-dates at least part of the deformation of the Silica Nappe.

4. Magnetic stratigraphy

The HBT magnetization components for the Lower Trench, Upper Trench and the quarry sections are plotted against stratigraphic distance to

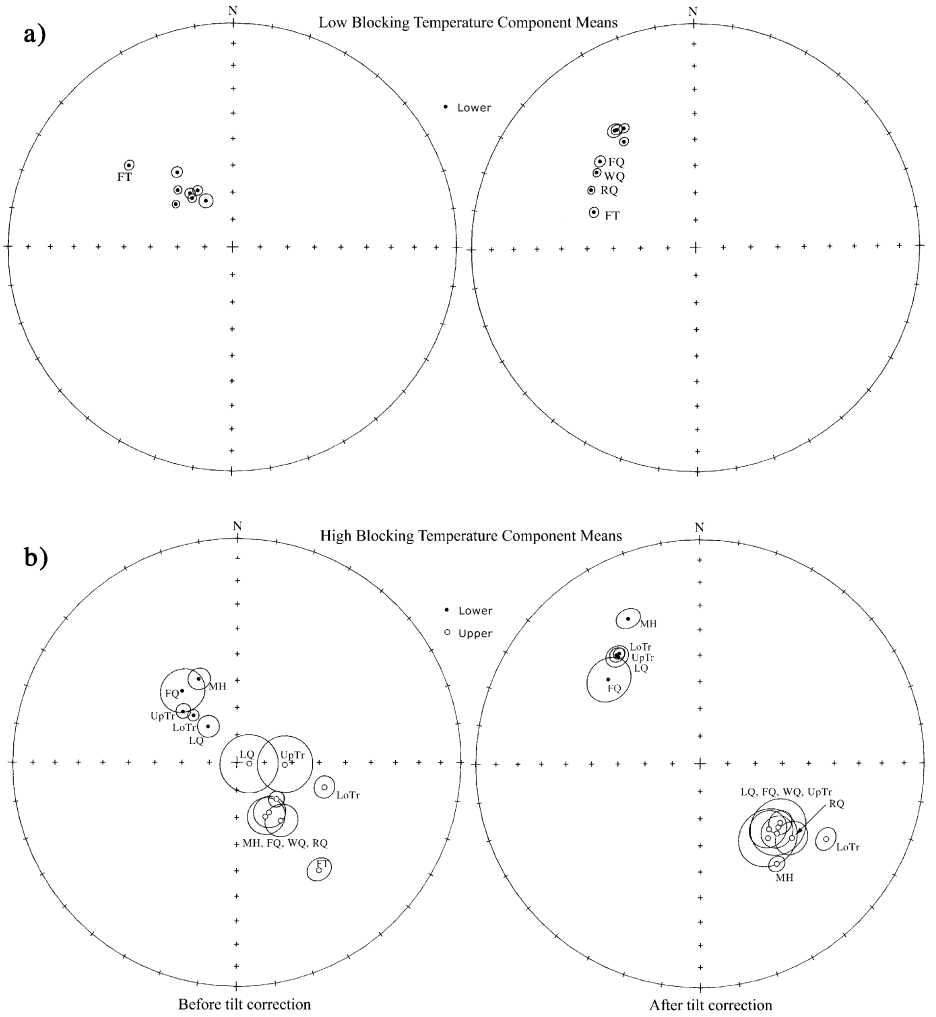

Fig. 7. Equal area projections of LBT site means (a) and HBT site means (b). Means are calculated separately for normal and reverse polarity directions from each site. Abbreviations: UpTr, Upper Trench; LoTr, Lower Trench; MH, Massiger Hellkalk Quarry; LQ, Lower Quarry; FT, Frontal Quarry; RQ, Right Quarry; WQ, West Quarry; FT, Fold Test Quarry. Closed and open symbols represent downward and upward inclinations, respectively.

produce the magnetic stratigraphy (Figs. 8–11; Tables 1 and 2). Data from the Fold Test Quarry are not plotted as it has the same age as the Right Quarry and is entirely reverse polarity. For the Lower Trench (Fig. 8) and the quarry sections (Figs. 10 and 11), the maximum angular deviation (MAD) values (see Kirschvink, 1980) are generally below 15° indicating that the HBT components are adequately defined. For the Upper Trench (Fig. 9), the MAD values are high ($>15°$) at the top of the section indicating that the HBT component is poorly defined in this part of the section. MAD values of zero in reverse polarity intervals of the Upper Trench (Fig. 9) indicate that the (reverse) component could not be defined by the standard principal component analysis (Kirschvink, 1980) due to poorly defined decay of the magnetization vector during thermal demagnetization. In these cases, we resorted to use of a 'stable end-point' to determine the HBT

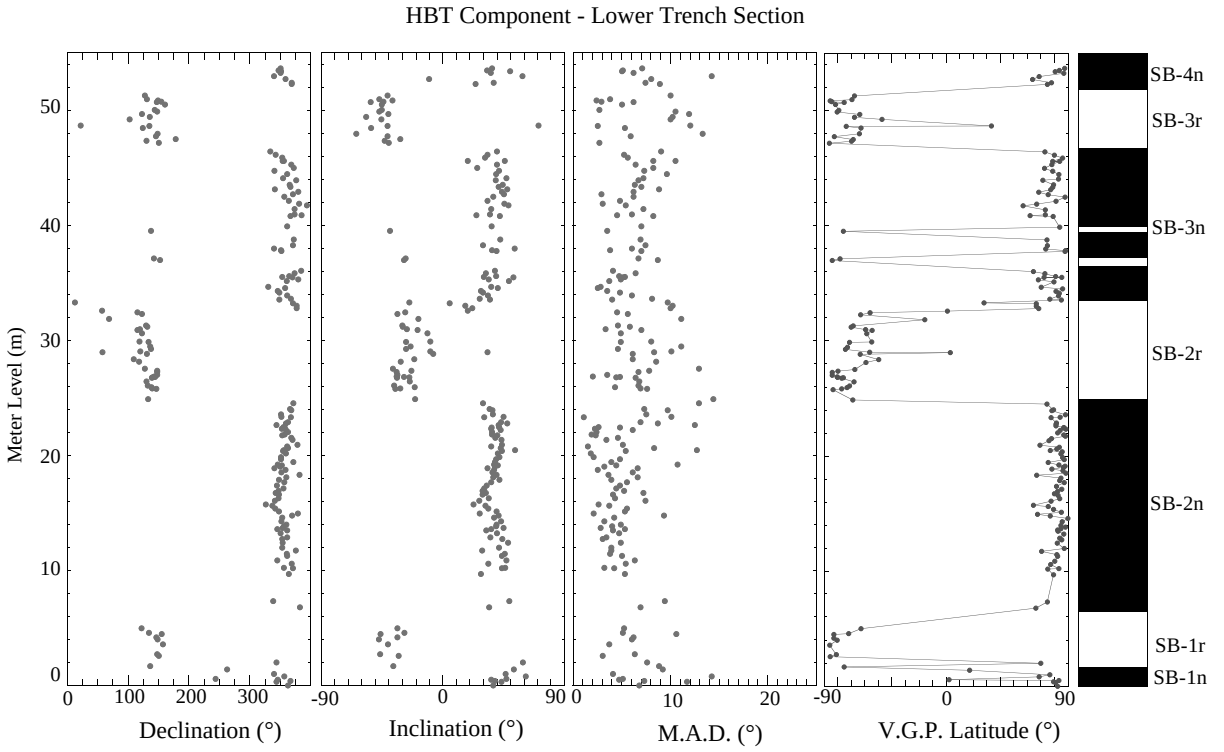

Fig. 8. Component declination, inclination, MAD values, VGP latitudes and polarity interpretation for the HBT magnetization component from the Lower Trench.

component anchoring the stable-end point to the origin of the orthogonal projection and determining the direction represented by this line.

Polarity zones were based on the virtual geomagnetic polar (VGP) latitudes derived from the HBT component directions (Figs. 8–11). We use a sequential numbering of polarity zones from the base of the composite section with a prefix SB (Silická Brezová) (Fig. 12). The correlation of the Lower Trench to the Massiger Hellkalk Quarry is based on the facies transition at the base of the Massiger Hellkalk Unit and by con-

Table 1
Mean LBT magnetization directions

	Before tilt correction					After tilt correction			
	N	Dec (°)	Inc (°)	k	α_{95} (°)	Dec (°)	Inc (°)	k	α_{95} (°)
Lower Trench	280	320.3	66.9	27.4	1.6	326.5	42.3	27.4	1.6
Upper Trench	149	321.7	64.5	32.7	2.0	326.7	36.2	31.6	2.1
Massiger Hellkalk Unit	102	328.2	65.7	50.2	2.0	329.5	37.8	60.0	1.8
Lower Quarry	46	329.9	70.6	68.6	2.6	325.9	36.6	68.7	2.6
Frontal Quarry	104	323.3	55.7	49.3	2.0	312.6	42.0	47.8	2.0
Right Quarry	25	307.0	64.1	407.9	1.4	299.4	45.8	405.6	1.4
West Quarry	36	316.1	61.1	219.3	1.6	307.8	43.9	255.0	1.5
Fold test Quarry	45	308.3	40.8	124.5	1.9	289.7	50.3	137.5	1.8
Conglomerate test	31	314.7	71.9	134.2	2.2	323.7	42.4	134.2	2.2
Overall Mean (ex. Cong. Test)	8 sites	318.2	61.5	64.1	7.0	315.8	42.7	47.7	8.1

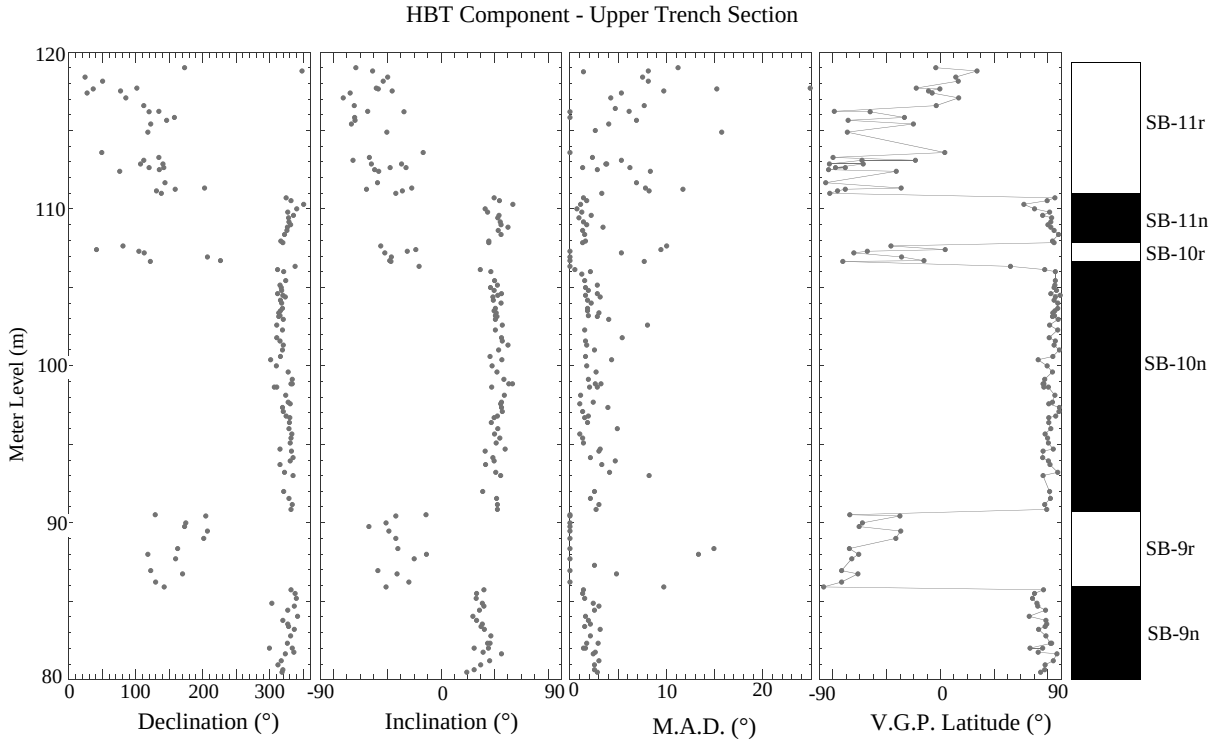

Fig. 9. Component declination, inclination, MAD values, VGP latitudes and polarity interpretation for the HBT magnetization component from the Upper Trench. MAD values of zero indicate that the component direction was calculated using the projection of a 'stable end-point' to the origin of the orthogonal projection.

odonts, and is consistent with the magnetostratigraphic correlation (Fig. 12). The correlation of the Massiger Hellkalk Quarry to the other quarries is based on physical tracing of individual beds from one quarry to another (Figs. 2 and 12). We have no correlation from the uppermost quarry section (West Quarry) to the Upper Trench, as there is an unsampled stratigraphic interval above the top of the uppermost quarry section where exposure is poor.

5. Conodont stratigraphy

Conodont taxonomy and the conodont zonation have been revised on the basis of detailed sampling of sections surrounding Silická Brezová and comparison with other Tethyan conodont stratigraphies. The description of new species, revision of the Upper Carnian to Upper Norian conodont genera, and discussion of the stratigraphically important species will be discussed elsewhere (Kozur et al., in press).

All Tethyan conodont zones from the base of Upper Carnian to the middle *Epigondolella triangularis–Norigondolella hallstattensis* Zone (upper Lower Norian), and from the Upper Alaunian *Mockina postera* Zone up to the top of the Norian (top Sevatian) are present in stratigraphic sequence at Silická Brezová (Fig. 2). The Upper Lacian and Alaunian Tethyan conodont zones between these intervals are also present but in the brecciated part of the section where the exposure is not suitable for magnetostratigraphic studies. There, the conodont index forms occur together with conodonts from the Lower Norian *Epigondolella abneptis* and *E. triangularis–N. hallstattensis* zones implying significant reworking in this part of the section (Figs. A1–A3).

The reference conodont zonation (after Kozur,

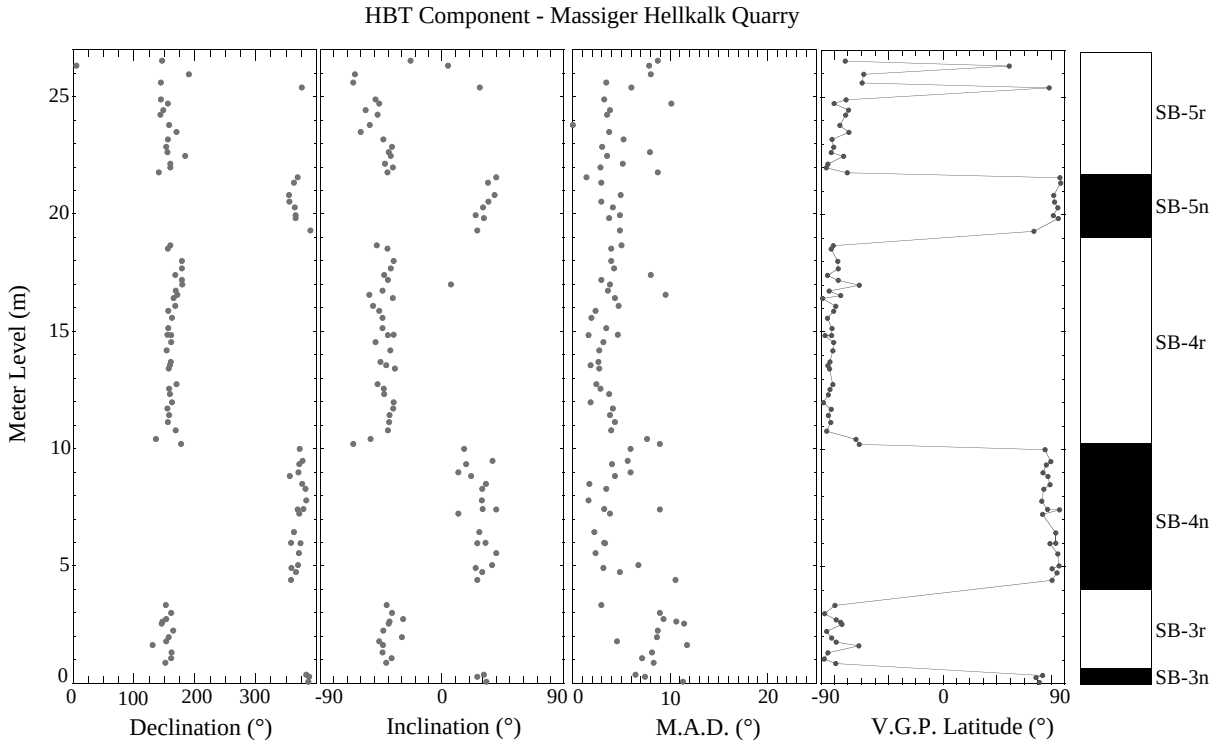

Fig. 10. Component declination, inclination, MAD values, VGP latitudes and polarity interpretation for the HBT magnetization component from the Massiger Hellkalk Quarry.

1980, 1996, 1999a,b; Krystyn, 1980; Budurov and Sudar, 1990; Kozur and Mock, 1991; Orchard, 1991a,b; Orchard and Tozer, 1997; Kozur et al., in press) is that given in Fig. 13. Ranges of index conodonts at Silická Brezová are given in Fig. 2. Some remarks are necessary on the conodont/ammonite zones and their correlations (Fig. 13), as they affect bio–magnetostratigraphic correlation among the Tethyan sections discussed below.

The boundary between the *Paragondolella carpathica* and *Epigondolella nodosa* zones, as used here, is different from the boundary between these two zones used by Krystyn in Gallet et al. (1994, 2000). This is caused by differences in the separation of *P. carpathica* and *E. nodosa*. We regard forms with small denticles or nodes on the transition between the unreduced platform and the rudimentary platform, and very indistinct nodes on the anterior part of the unreduced platform, as advanced *P. carpathica*. No *Epigondolella* has small nodes or denticles on the transition between the unreduced platform and the rudimentary platform. Krystyn regards such forms as primitive *E. nodosa* and therefore the *E. nodosa* Zone is expanded into our upper *P. carpathica* Zone. We regard as *E. nodosa* only forms in which the transition between the unreduced platform and the rudimentary platform is smooth and at least the anterior part of the unreduced platform has distinct nodes. For this reason our *E. nodosa* Zone begins in the middle–upper part of the lower *E. nodosa* Zone of Krystyn (and therefore of Gallet et al., 1994, 2000). The difference in separation of *P. carpathica* from *E. nodosa* is also seen in the conodont distribution of Gallet et al. (1994). Here, *P. carpathica* disappears at the level where *E. nodosa* appears. In our sections, advanced *P. carpathica* range up to close to the top of the *E. nodosa* Zone, as also reported by Muttoni et al. (2001) for Pizzo Mondello, Sicily.

The '*Metapolygnathus communisti*' Zone of North America cannot be directly correlated

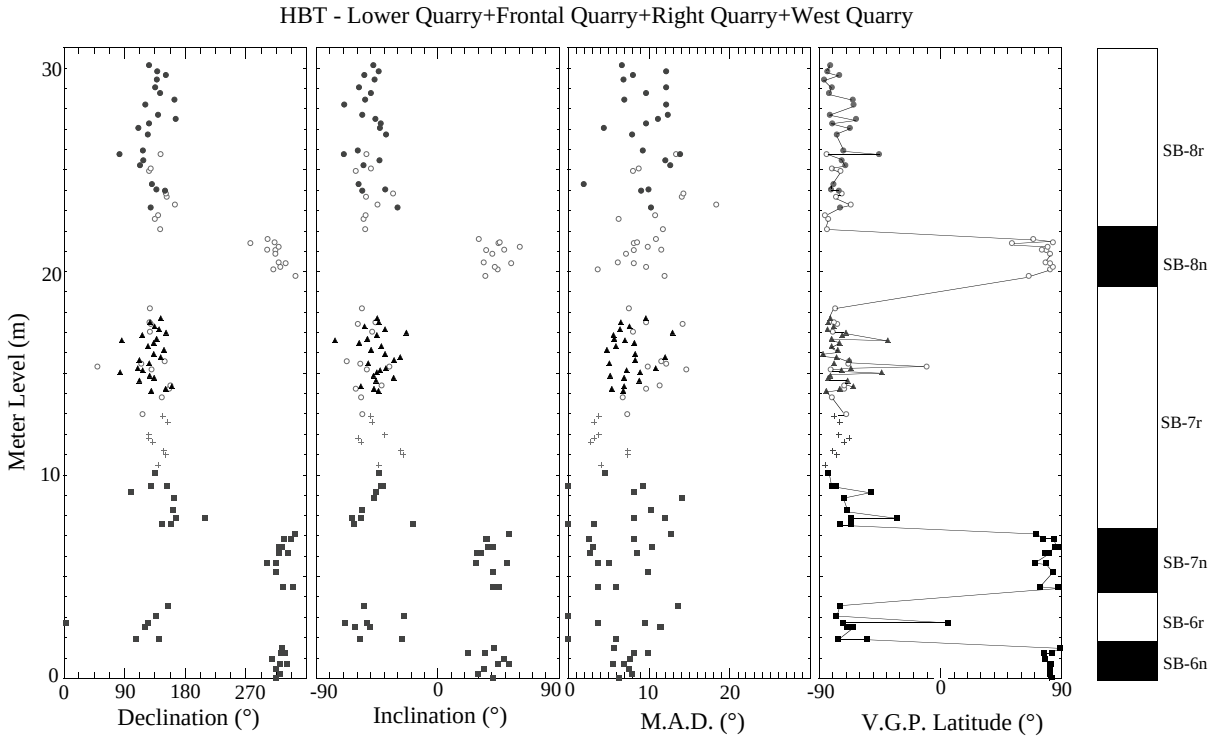

Fig. 11. Component declination, inclination, MAD values, VGP latitudes and polarity interpretation for the HBT magnetization component from quarry sections (other than Massiger Hellkalk Quarry). Lower Quarry: closed squares; Right Quarry: closed triangles; Frontal Quarry: open circles; West Quarry: closed circles. Crosses represent data from blocks (float) between the Lower Quarry and Frontal Quarry (see Fig. 2).

with the Tethys because '*M. communisti*' sensu Orchard (1991a) often does not belong to the genus *Metapolygnathus*, but is an advanced *Paragondolella*. The real *Metapolygnathus communisti* and *Epigondolella pseudodiebeli* often exclude each other for unknown (facies) reasons but they occur roughly at the same stratigraphic level. For this reason, only one zone, the *M. communisti–E. pseudodiebeli* Zone is discriminated within the Upper Tuvalian (Fig. 13). Its upper boundary is defined by the first appearance datum (FAD) of *Epigondolella primitia*, both in Tethys and in North America. The base of the *M. communisti–E. pseudodiebeli* Zone of the Tethys and the top of the *E. samueli* Zone (upper *E. nodosa* Zone) of North America coincide (Fig. 13). It is possible that true *M. communisti* are also present in North America (Carter and Orchard, 2000) but they are not illustrated by Orchard (1991a,b). Orchard (1991a,b) mentioned a large intraspecific variability in this species. However, the true *M. communisti* from the western margin of the Pacific and Tethys has a low intraspecific variability. If, however, '*M. communisti*' sensu Orchard (1991a) and true *M. communisti* were put in one species, then, except for the delicate sculpture, all features would be extremely variable.

The Carnian–Norian boundary is not yet fixed either in chronostratigraphy or in conodont biostratigraphy. For many years, there was an agreement between Tethyan and North American researchers to use the FAD of *Norigondolella navicula* in the middle part of the *Epigondolella primitia* Zone to mark the base of the Norian. Krystyn (1980) first advocated this definition for the base of the Norian. In the Neotethys, however, *N. navicula* is very rare and often missing (e.g. in the Pizzo Mondello section, Muttoni et al., 2001). Orchard et al. (2000) have made the case that the FAD of *N. navicula* is characterized

Table 2
Mean HBT magnetization directions

	Before tilt correction					After tilt correction			
	N	Dec (°)	Inc (°)	k	α_{95} (°)	Dec (°)	Inc (°)	k	α_{95} (°)
Lower Trench (N+R)	200	304.3	61.0	18.2	2.4	316.1	38.0	17.5	2.4
Lower Trench (N)	139	313.8	62.2	20.2	2.7	322.8	38.8	20.1	2.7
Lower Trench (R)	61	105.7	−56.1	23.0	3.9	121.1	−34.9	23.4	3.9
Upper Trench (N+R)	142	306.4	69.4	10.2	3.9	320.1	43.4	10.8	3.8
Upper Trench (N)	94	317.0	66.6	36.4	2.5	323.8	38.9	49.3	2.1
Upper Trench (R)	48	92.1	−72.5	4.7	10.6	129.3	−52.9	4.9	10.2
Massiger Hellkalk (N+R)	91	143.6	−65.9	29.4	2.8	147.2	−38.0	29.4	2.8
Massiger Hellkalk (N)	32	335.5	56.3	41.6	4.0	333.8	28.4	41.7	4.0
Massiger Hellkalk (R)	59	132.9	−70.4	41.0	2.9	142.8	−43.0	41.0	2.9
Lower Quarry (N+R)	39	314.0	79.3	18.0	5.5	320.6	45.4	18.0	5.5
Lower Quarry (N)	17	321.4	73.3	53.1	4.4	322.4	39.3	53.0	4.4
Lower Quarry (R)	22	96.5	−85.6	11.6	10.6	137.7	−52.9	11.6	10.6
Frontal Quarry (N+R)	33	147.4	−63.8	23.3	5.3	133.6	−51.0	23.3	5.3
Frontal Quarry (N)	12	322.8	56.9	33.3	7.6	312.8	43.8	30.4	8.0
Frontal Quarry (R)	21	151.3	−67.7	22.3	6.9	134.1	−55.2	23.1	6.8
Right Quarry (R)	24	142.5	−63.3	24.9	6.0	129.3	−46.5	24.9	6.0
West Quarry (R)	21	146.6	−68.4	29.6	5.9	131.8	−52.1	30.7	5.8
Fold test Quarry (R)	45	142.4	−39.5	23.7	4.5	126.4	−53.4	25.7	4.3
Quarries combined (N+R)	162	143.0	−61.4	13.3	3.2	132.6	−50.0	22.0	2.4
Quarries combined (N)	33	322.1	67.4	31.6	4.5	319.1	41.0	39.0	4.1
Quarries combined (R)	129	143.2	−59.8	11.8	3.8	130.6	−52.2	21.8	2.7
Conglomerate test	10 clasts	12.1	54.8	3.0	34.0	356.5	29.5	3.0	34.0
Overall Mean (ex. Cong. Test)	8 sites	319.1	64.1	46.4	8.2	316.1	46.2	112.5	5.2
						Pole Lat. 50.3N Pole Long. 274.3E dp/dm = 4.3/6.7			

by abrupt onset of mass occurrence of this species and is therefore partly facies controlled. Although the FAD of *N. navicula* is not ideal for defining the base of the Norian, this definition is used at Silická Brezová and in our correlation charts. At Silická Brezová, the FAD of *N. navicula* is very easily recognized and this event has been used in most conodont papers since Krystyn (1980).

Krystyn in Gallet et al. (1992, 1994, 2000) used the FAD of *Metapolygnathus communisti* B for definition of the base of the Norian. This taxon is neither a *M. communisti* nor a *Metapolygnathus* and has still to be described. In the trench section at Silická Brezová, this form is sporadically present and its FAD is a slightly below the FAD of *Norigondolella navicula*. In other Tethyan outcrops, this taxon is either absent or the FAD is close to the FAD of *N. navicula*. In all sections where this species is present, it is very rare and occurs sporadically. It is a homoeomorph form to *Epigondolella nodosa* (with only few minor differences), however, because of its occurrence in the Lower Norian, it is not directly related to *E. nodosa*. *Paragondolella oertlii* (Kozur) is probably its forerunner. In North America, '*M. communisti* B' is absent. This fact, and the sporadic occurrence of '*M. communisti* B' in the Tethys makes the FAD of '*M. communisti* B' unsuitable for definition of the base of the Norian. The fact that the FAD of '*M. communisti* B' is close to the FAD of *N. navicula* allows approximate placement of the base of the Norian in Gallet et al. (1992, 1994, 2000). Orchard et al. (2000) proposed the base of the Norian at the base of the '*M. communisti* Zone' (for problems with the North American *M. communisti* Zone, see above), however, the

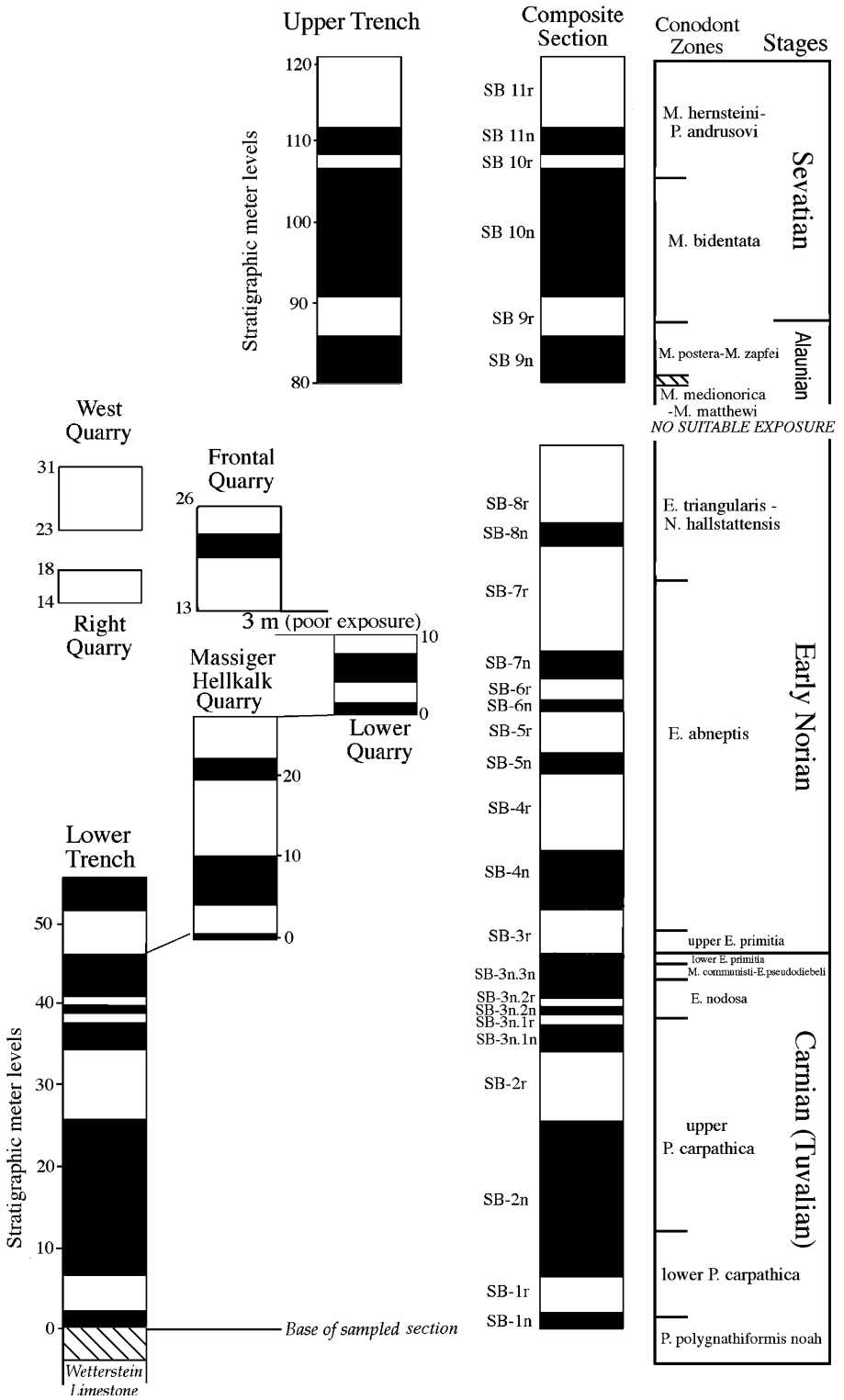
Upper Trench
Stratigraphic meter levels
120
110
100
90
80
Composite Section
SB 11r
SB 11n
SB 10r
SB 10n
SB 9r
SB 9n
Conodont Zones
Stages
M. hernsteini-
P. andrusovi
M. bidentata
Sevatian
M. postera-M. zapfei
Alaunian
M. medionorica
-M. matthewi
NO SUITABLE EXPOSURE
West Quarry
31
23
18
14
Right Quarry
Frontal Quarry
26
13
3 m (poor exposure)
10
0
Massiger Hellkalk Quarry
Lower Quarry
20
10
0
Lower Trench
50
40
30
20
10
0
Stratigraphic meter levels
Base of sampled section
Wetterstein Limestone
SB-8r
SB-8n
SB-7r
SB-7n
SB-6r
SB-6n
SB-5r
SB-5n
SB-4r
SB-4n
SB-3r
SB-3n.3n
SB-3n.2r
SB-3n.2n
SB-3n.1r
SB-3n.1n
SB-2r
SB-2n
SB-1r
SB-1n
E. triangularis -
N. hallstattensis
E. abneptis
Early Norian
upper E. primitia
lower E. primitia
M. communisti-E.pseudodiebeli
E. nodosa
upper
P. carpathica
lower P. carpathica
P. polygnathiformis noah
Carnian (Tuvalian)

Stage		Substage Cordevolian	Ammonoid Zone/Subzone Standard		Conodont Zone/Subzone Tethys/Western Pacific		North America	
Upper Triassic	Rhaetian	Upper Rhaetian	Chor. marshi	*Choristoceras marshi*	*Misikella ultima*		*Norigondolella sp.*	
				Chorist. ammonitiforme	*Misikella posthernsteini*	*Misikella koessenensis*	*Misik. posthernsteini*	
		Lower Rhaetian	"Ch." haueri	*Vandaites stuerzenbaumi*			*Mockina mosheri*	
				Choristoceras haueri		*Misikella hern= steini-Misikella posthernsteini*		
			Cochloceras suessi					
	Norian	Sevatian	*Sagenites reticulatus*		*M. hernsteini-P. andrusovi*		*Mockina bidentata*	
			Sagenites quinquepunctatus		*Mockina bidentata*	Subzone 2		
			Halorites macer			Subzone 1		
		Alaunian	*Mesohimavatites columbianus*		*Mockina postera*		*Mockina serrulata*	
							Mockina postera	
							Mockina elongata	
					Epigondolella spiculata		*Epigondolella spiculata*	
			Cyrtopleurites bicrenatus		*M. matthewi-M. medionorica*		*Mockina multidentata*	
		Lower Norian	*Juvavites magnus*		*Epigondolella triangularis-Norigondolella hallstattensis*		*Epigondolella triangularis*	
			Malayites paulckei		*Epigondolella abneptis*		*Epigondolella abneptis*	
			Stikinoceras kerri		*Epigondolella primitia*	upper	*Epigondolella primitia*	upper
						lower		lower
	Carnian	Tuvalian	*Klamathites macrolobatus*		*Metapolygnathus communisti-Epigondolella pseudodiebeli*		*Metapolygn. communisti*	
			Tropites welleri		*Epigondolella nodosa*		*Epigondolella nodosa*	upper
					Paragondolella carpathica	upper		middle
						lower		lower
			Tropites dilleri		*Paragondolella polygnathiformis*		*Paragondolella polygnathiformis*	
		Julian	*Austrotrachyceras austriacum*		*Gladigondolella tethydis-Paragondolella polygnathiformis*			
			Trachyceras aonoides					
		Cordevolian	*Trachyceras aon*		*Budurovignathus diebeli-Paragondolella polygnathiformis*			
			D. canadiensis-F. sutherlandi					

Preferred base of Norian Generally used base of Norian

Fig. 13. Tethys/Western Pacific conodont zonation and its correlation to ammonoid zones.

occurrence of *M. communisti* is strongly facies controlled. *M. communisti* and contemporaneous *Epigondolella* species often exclude each other.

The most distinct change both in conodont and radiolarian faunas occurs at the base of the *Epigondolella abneptis* Zone which would be a very good alternative definition for the base of the Norian (Fig. 13). It lies within the *Stikinoceras kerri* ammonoid Zone but close to the upper boundary of this zone (upper part of *kerri* Zone II). The base of the *E. abneptis* Zone corresponds closely to the appearance of *Halobia styriaca* (Krystyn, 2002). The *E. abneptis* Zone is well defined by the FAD of *E. abneptis* both in the Tethys and in North America. As *E. quadrata* Orchard (= *E. vialovi* Burij) is a junior synonym of *E. abneptis*, the name *E. quadrata* Zone is replaced by the name *E. abneptis* Zone.

Fig. 12. Polarity record from the individual sections, and the composite section, at Silická Brezová. Black: normal polarity. White: reverse polarity.

The base of the *Epigondolella triangularis–Norigondolella hallstattensis* Zone is defined by the FAD of *N. hallstattensis* because *E. triangularis* is rare to very rare in the lower *E. triangularis* Zone, where *Epigondolella abneptis* dominates as in the underlying *E. abneptis* Zone. If the samples are not rich in conodonts, it is difficult to separate the *E. triangularis–N. hallstattensis* Zone from the *E. abneptis* Zone on the basis of the occurrence of *E. triangularis*. However, at this level *N. hallstattensis* is very common. It begins only just below the FAD of typical *E. triangularis*.

The base of the *Epigondolella triangularis–Norigondolella hallstattensis* Zone used by Krystyn and therefore also in the papers by Gallet et al. (1992, 1993) is defined by *Epigondolella abneptis* with distinct widening of the posterior platform which bears, however, no denticles. These forms, included in *E. abneptis spatulata* in Krystyn (1980) and subsequently in *E. triangularis*, do not fit in the definition of *E. triangularis* and are typical forms of the *E. abneptis* Zone. In Muttoni et al. (2001) similar forms were labelled as *Epigondolella spatulata*, a species that occurs only in the upper part of the *E. triangularis–N. hallstattensis* Zone or in an independent *E. spatulata* Zone above the *E. triangularis–N. hallstattensis* Zone as discriminated by Gallet et al. (1993). For this reason, the lower half of the *E. triangularis–N. hallstattensis* Zone in Gallet et al. (1992, 1993) and the entire investigated *E. triangularis* Zone at the Pizzo Mondello section (Muttoni et al., 2001) belong to the *E. abneptis* Zone. The *E. triangularis–N. hallstattensis* Zone sensu Kozur (1989, 1997), used in this paper, corresponds to the *E. triangularis* Zone used by Orchard (1991b). Krystyn (in Gallet et al., 1993, 2000) made sound arguments for designating an independent *E. spatulata* Zone within the present upper *E. triangularis–N. hallstattensis* Zone. As the *E. spatulata* fauna occurs in Silická Brezová in the sedimentologically complicated part (brecciated interval with reworking), we cannot resolve this question from our material. To facilitate correlation with the North American conodont zonation, we provisionally include the *E. spatulata* Zone in the upper *E. triangularis–N. hallstattensis* Zone, following Orchard (1991a,b).

As pointed out by Orchard (1991a) and discussed by Kozur et al. (in press), the North American '*Mockina*' *multidentata* lineage has not been found in the Tethys. '*E.*' *multidentata* or '*E.*' cf. *multidentata* sensu Krystyn belongs to another species, *Mockina medionorica* n. sp., which is transitional between *M. matthewi* and *Mockina* of the *M. postera* group. *M. matthewi* is rarely present in the Tethys. These two species define the interval of the '*M.*' *multidentata* Zone of North America because they are situated between the top of the *Epigondolella triangularis–Norigondolella hallstattensis* Zone (including the *E. spatulata* Zone sensu Krystyn) and the base of the '*Epigondolella*' *spiculata* fauna, which are both present in the Tethys and in North America. However, in the Tethys, *E. abneptis* and *E. triangularis* have a longer range than in North America and extend into the lower part of the Middle Norian (Alaunian). It has been difficult to define the upper range of *Epigondolella abneptis* and *E. triangularis* in the Tethys. In the upper *M. postera–M. zapfei* Zone, they are probably no longer present.

Kozur (1996) defined the base of the Rhaetian with the FAD of *Misikella posthernsteini*. This boundary is recognizable throughout the Tethys and in the western Pacific region. In North America, Kozur (1996) defined the base of the Rhaetian by the base of the '*Mockina*' *mosheri* Zone that coincides with the base of the *Cochloceras amoenum* ammonoid Zone. The FAD of *M. posthernsteini* is either at the base of the *Cochloceras suessi* ammonoid Zone or in its lowermost part. *M. posthernsteini* occurs in the *C. suessi* Zone in red Hallstatt Limestone facies in the Northern Alps (Kozur, 1996). *Cochloceras* in red Hallstatt Limestones represents the lowermost *C. suessi* Zone. For this reason, the base of the *M. posthernsteini* Zone can be roughly correlated with the base of the *C. suessi* ammonoid zone. As both the base of the *C. suessi* Zone and the base of the *M. posthernsteini* Zone represent a strong faunal turnover (e.g. disappearance of *Monotis*, appearance of several Rhaetian guide forms of radiolarians, distinct changes in the holothurian faunas), it is probable that the bases of both zones coincide. Orchard and Tozer (1997) discriminated the '*M.*' *mosheri* Zone and, like Kozur (1996), defined

the base of the Rhaetian in North America using the base of the '*M.*' *mosheri* Zone and the contemporaneous base of the *C. amoenum* ammonoid zone. Gallet et al. (1996) regarded the *C. suessi* Zone as part of their Sevatian 2.

The exact correlation of the conodont zonation between the different biomagnetostratigraphically investigated Tethyan marine sections is hampered by the fact that certain important marker species were not reported from, or are not present in, sections in Austria, Sicily and Turkey. This is particularly the case around the Carnian–Norian boundary. The correlations are presented in Fig. 14.

6. Bio- and magnetostratigraphic correlation of Silická Brezová and Pizzo Mondello (Sicily)

Some of the stratigraphically important conodonts of the Pizzo Mondello section (Muttoni et al., 2001) are incorporated into a photographic plate. Unfortunately, *Norigondolella navicula* is not present in this section, making the recognition of the Carnian–Norian boundary difficult. In the Upper Tuvalian to Lower Lacian time interval, there are several ranges and co-occurrences of conodonts that are unique to Pizzo Mondello and not found elsewhere. Pizzo Mondello samples PM0–PM12 (Muttoni et al., 2001) belong to the middle and upper *Epigondolella nodosa* Zone which comprises the upper *E. nodosa zoae* and *E. samueli* zones of North America (Fig. 13). This is indicated by an advanced *E. nodosa* with platform denticles rather than nodes (sample PM1). Such forms are not present in the lower *E. nodosa* Zone. The base of the overlying *Metapolygnathus communisti–Epigondolella pseudodiebeli* Zone is defined by the FAD of *M. communisti* in sample PM13. The overlying sample PM14 also belongs to this zone, as it has the same conodont fauna. Up to sample PM18, *Paragondolella polygnathiformis noah* and *P. carpathica* are present. This normally indicates an age not younger than the *M. communisti–E. pseudodiebeli* Zone, but additionally *Epigondolella primitia* is indicated, the guideform of the next younger conodont zone which by definition does not occur in the *M. communisti–E. pseudodiebeli* Zone. Sample PM27 and younger beds are Lower Norian. A very advanced *M. communisti*, indicated by the rather well developed platform nodes, is illustrated from sample PM27. Such forms occur only in the Lower Norian range of *M. communisti*, especially around the boundary of the *E. primitia* and *Epigondolella abneptis* zones. The interval between samples PM19 and PM26 cannot be clearly dated by specified conodont ranges and illustrated conodonts. However, as discussed below, by combination of the conodont and paleomagnetic data, the Carnian–Norian boundary defined by the FAD of *N. navicula* within the *E. primitia* Zone can be well determined.

Polarity zone PM4r at Pizzo Mondello (Muttoni et al., 2001) corresponds to SB-3r (Fig. 14). This would mean that the base of the Norian defined by the FAD of *Norigondolella navicula* within the *Epigondolella primitia* Zone at Silická Brezová would be between samples PM25 and PM26, within the uppermost part of polarity zone PM4n. From Sample PM26 a moderately advanced *E. primitia* is illustrated which would fit well in the middle part of the *E. primitia* Zone, close to the Carnian–Norian boundary. As mentioned above, in the next higher sample (PM27), an advanced Lower Norian type of *Metapolygnathus communisti* is illustrated.

The top of polarity zone SB-3r lies a little above the base of the *Epigondolella abneptis* Zone and correlates to the top of PM4r that lies at the last appearance datum (LAD) of *Metapolygnathus communisti* in sample PM28 and somewhat below the LAD of *Epigondolella primitia* in sample PM30. This would mean, however, that *E.* '*quadrata*' (*E. abneptis*) mentioned from samples PM23–PM26 would not be *E. abneptis*, but any other species of the *E. abneptis* group, e.g. *E. permica* (Hayashi) or *E. pseudoechinata* Kozur, that occur below the *E. abneptis* Zone. Polarity zones PM5n to PM6n correspond to SB-4n. The thin zone PM5r was not found in the Hallstatt Limestones of Silická Brezová presumably because of their low sedimentation rate. Polarity zone PM6r corresponds to SB-4r that lies within the *E. abneptis* Zone. At Pizzo Mondello, the interval from the middle part of PM5n to PM6r lies


NEWARK BASIN
FORM-ATION
STAGE
SUB-STAGE
Ma
200
205
210
215
220
225
230
undivided
Sevatian
Alaunian
Lacian
Tuvalian
RHAETIAN
NORIAN
CARNIAN
PASSAIC FORMATION
LOCKATONG FORMATION
STOCKTON FORMATION
Cycle
GPTS
E24
E23
E22
E21
E20
E19
E18
E17
E16
E15
E14
E13
E12
E11
E10
E9
E8
E7
E6
E5
E4
E3
E2
E1
SILICKÁ BREZOVÁ
Composite Section
NOT STUDIED
SB-11r
SB-11n
SB-10n
SB-9r
SB-9n
SB-8r
SB-8n
SB-7r
SB-7n
SB-6r
SB-6n
SB-5r
SB-5n
SB-4r
SB-4n
SB-3r
SB-3n.3n
SB-3n.2r
SB-3n.2n
SB-3n.1r
SB-3n.1n
SB-2r
SB-2n
SB-1r
SB-1n
20 m
Scheiblkogel (Gallet et al., 1996)
Rhaet.
Sevatian
Alaunian
S-5n
S-4r
S-4n
S-3r
S-3n
S-2r
S-2n
S-1r
1m
Pizzo Mondello (Muttoni et al., 2001)
20 m
Lacian
Tuvalian
PM6r
PM5n
PM4n
PM3n
PM2r
PM2n
PM1
Kavalani (Gallet et al., 2000)
Sevatian
Alaunian
Lacian
Tuvalian
KV-19
KV-18
KV-15
KV-13
KV-12
KV-10
KV-7
KV-6
KV-5
KV-3
KV-2
KV-1
10 m
Erenkolu Mezardik (Gallet et al., 1994)
Tuvalian
LAC.1
M-
L+
K-
J+
I-
H+
1 m
Kavur Tepe (Gallet et al., 1993)
Sevatian
Lacian
I-
H+
G-
F+
E-
D+
B+
A-
5 m
Bolücektasi Tepe (Gallet et al., 1992, 2000)
Alaunian
Lacian
BT-10r
BT-10n
BT-9n
BT-8n
BT-7r
BT-7n
BT-6n
BT-4r
BT-4n
5 m
Bolücektasi Tepe (Gallet et al., 1994)
Lacian
Tuvalian
BT-4n
BT-3r
BT-3n.2n
BT-2r
BT-2n
BT-1r
BT-1n
1 m
SILICKÁ BREZOVÁ
Polarity
Conodont Zones
Sub-stage
Sevatian
Alaun.
Early Norian (Lacian)
Carnian (Tuvalian)
M. hernsteini-P. andrusovi
M. bidentata
M. postera-M. zapfei
M. medionorica-M. matthewi
NO SUITABLE EXPOSURE
E. triangularis-N. hallstattensis
E. abneptis
upper E. primitia
lower E. primitia
M. communisti-E. pseudod.
E. nodosa
upper P. carpathica
lower P. carpathica
P. polygnathiformis noah

within the range of *E. triangularis* (*E. triangularis* Zone). At Silická Brezová this interval (middle part of SB-4n and SB-4r) lies within the *E. abneptis* Zone. The only two illustrated conodonts from this interval in Pizzo Mondello are *E. quadrata* (= *E. abneptis*) from the lowermost part of this interval (sample PM33), and *E. spatulata* from the top of this interval (sample PM45). *E. spatulata* is restricted to the uppermost part of the *E. triangularis* Zone or *E. spatulata* Zone (sensu Krystyn) above the *E. triangularis* Zone. However, the illustrated form has a triangular platform, in which the posterior widened part has no nodes or denticles. It is, therefore, not an *E. spatulata*, in which the widened posterior part of the platform has marginal denticles or nodes, but it belongs to *E. abneptis*. Such morphotypes of *E. abneptis* are especially common in the middle and upper part of the *E. abneptis* Zone, but rarely occur in the lower *E. abneptis* Zone.

The *Metapolygnathus communisti–Epigondolella pseudodiebeli* Zone and the lower *E. primitia* Zone at Pizzo Mondello have predominantly normal polarity (PM3n and PM4n) subdivided by a thin reverse polarity interval, PM3r. The normal polarity interval PM3n extends downward into the very much expanded *E. nodosa* Zone. In Silická Brezová, the entire interval from the upper *E. nodosa* Zone to the lower *E. primitia* Zone has normal polarity (SB-3n.3n). The thin reverse polarity interval PM3r was not found in Silická Brezová. The *M. communisti–E. pseudodiebeli* Zone and the lower *E. primitia* Zone are condensed at Silická Brezová, indicating low sedimentation rates and there is possibly a short gap in the *M. communisti–E. pseudodiebeli* Zone. In the section adjacent to the new quarries that was investigated in several papers by Kozur and Mock (Kozur, 1972; Kozur and Mock, 1974a,d; Mock, 1980), *M. communisti* is very common, mainly represented by juvenile forms described as *M. parvus*. In this quarry, the specimens occur in a layer a few tens of centimeters thick, whereas other layers of the *M. communisti–E. pseudodiebeli* Zone are characterized by *E. pseudodiebeli* and *E. pseudoechinatus*. In the trench section, this part of the section was densely sampled (about 10-cm sampling interval), but no horizon with *M. communisti* was found. Thus, a short gap within the *M. communisti–E. pseudodiebeli* Zone is probably present although *M. communisti* and *E. pseudodiebeli* tend to exclude each other for unknown facies reasons.

In the *Epigondolella nodosa* Zone the correlation between Silická Brezová and Pizzo Mondello is not compelling, possibly due to variable sedimentation rates in the calciturbidites of the Pizzo Mondello section. The sedimentation rate is apparently very low in the middle and upper *E. nodosa* Zone of the trench section at Silická Brezová (Fig. 15), but very high and probably strongly variable at this level of the Pizzo Mondello section. In the trench section the upper *E. nodosa* Zone is within SB-3n.3n. In the middle *E. nodosa* Zone the reverse polarity zone SB-3n.2r may correspond to the thicker reverse polarity zone PM2r. In view of the thick interval comprising the middle and upper *E. nodosa* Zone at Pizzo Mondello, PM2r may be of comparable duration to SB-3n.2r. Polarity zone SB-3n.2n corresponds to the PM1n–PM2n interval. The intervening PM1r occurs in the very rapidly deposited part of the Pizzo Mondello section and is missing within SB-3n.2n at Silická Brezová where sedimentation rates are very low (Fig. 15).

Muttoni et al. (2001) indicated a possible Carnian–Norian boundary interval from 66 to 106 m at Pizzo Mondello. At Silická Brezová, the Carnian–Norian boundary, as defined by the FAD of *Norigondolella navicula*, can be fixed to the centimeter level. Taking into consideration the possibility of variable sedimentation rates and the

Fig. 14. Correlation of the Silická Brezová composite section to the Newark Basin (Kent and Olsen, 1999, 2000) and the marine sections in Turkey and Scheiblkogel, Austria (Gallet et al., 1992, 1994, 1996, 2000), and Pizzo Mondello, Sicily (Muttoni et al., 2001). The stratigraphic stage boundaries in the Tethyan marine sections and the Newark Basin have been re-assigned (see text). An age of 200 Ma for the Triassic–Jurassic boundary is adopted from Pálfy et al. (2000, 2002). The Newark polarity stratigraphy and cyclostratigraphy are from Kent and Olsen (1999).

stratigraphic uncertainties, satisfactory correlation between Pizzo Mondello and Silická Brezová can be achieved (Fig. 14).

7. Bio- and magnetostratigraphic correlation of Silická Brezová with marine sections in Turkey and Austria

Gallet et al. (1992, 1993, 1994, 1996, 2000) have published bio–magnetostratigraphic investigations of Tethyan Upper Triassic sequences in Turkey and Austria. Despite the fact that only the conodont zones and/or the conodont ranges are given, but no illustrations are presented, the biostratigraphic correlation of the sections investigated by these authors with the Silická Brezová section is achievable. This is because of the fact that the taxonomic scope of the species used in these papers (determinations by Krystyn) corresponds in large part to that used in the present paper, and when this is not the case, the differences are known. Moreover, Krystyn (in Gallet et al., 2000) recognized *Epigondolella pseudodiebeli* in these sections and hence correlations around the Carnian–Norian boundary are facilitated. The conodont zonation used in the papers by Gallet et al. is partly the same as that used for Silická Brezová, but with a different boundary between the *Paragondolella carpathica* and *E. nodosa* Zones and the *E. abneptis* and *E. triangularis* Zones (explained above). The ranges of zones used by Gallet et al. (*E. spatulata* Zone, *E. slovakensis* Zone = *Epigondolella* n. sp. D Zone and *E. vrielyncki* Zone = *Epigondolella* n. sp. E Zone) can be unambiguously correlated with our conodont zonation. The exact position of the '*Metapolygnathus communisti* B Zone' is difficult to determine, because '*M. communisti* B' is rare and the FAD appears to have variable stratigraphic position, perhaps due to its rare occurrence and poorly defined taxonomic scope. For example, the FAD begins at Feuerkogel distinctly above the FAD of *Norigondolella navicula* (Krystyn, 1980), and at Silická Brezová slightly below the FAD of *N. navicula*.

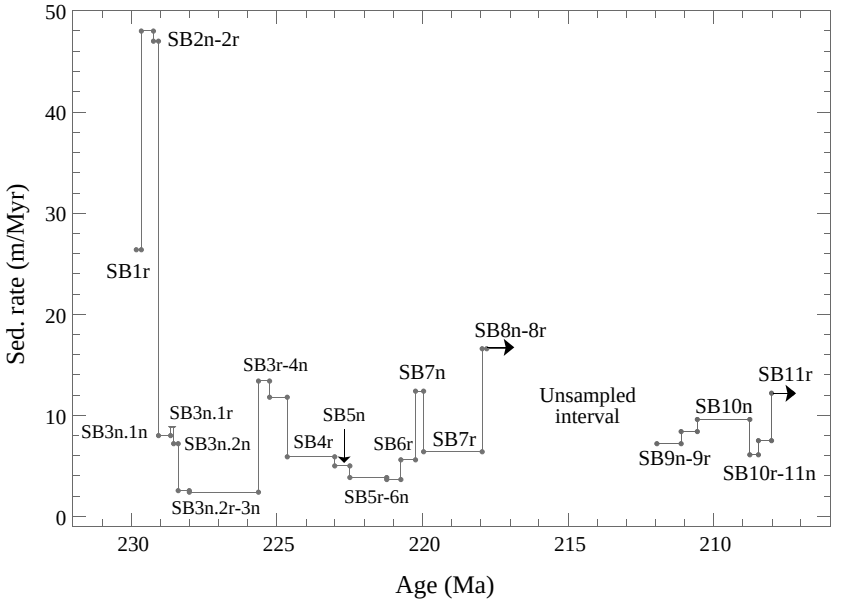

Fig. 15. Sedimentation rates for the Silická Brezová section based on our correlation to the Newark polarity stratigraphy, and the Newark basin chronology (Kent and Olsen, 1999). Note the high sedimentation rates in the bioclastic limestones (SB2n-2r) at the transition from the Wetterstein Limestone to the Hallstatt Limestone (see Fig. 2) and the very low sedimentation rates in SB3n in micritic limestones at the base of the Hallstatt Limestones.

7.1. Erenkolu Mezarlik Section, Antalya Nappes, Turkey

The Erenkolu Mezarlik section is situated in the Antalya Nappes close to Kemer (Gallet et al., 1994). It consists of an extremely condensed sequence of Hallstatt Limestones. Only 5 m of sediments comprises the Carnian and the basal part of the Norian, and only the upper part of the section (< 2 m) is correlative to Silická Brezová. The normal polarity zone H+ of the Erenkolu Mezarlik section corresponds to the upper part of SB-2n in Silická Brezová (Fig. 14). Both polarity zones lie within the *Paragondolella carpathica* Zone. The reverse polarity zone SB-2r in Silická Brezová lies within the upper *P. carpathica* Zone. In the Erenkolu Mezarlik section, the correlative polarity zone (I-) is in the upper *P. carpathica* Zone and in the lower part of lower *Epigondolella nodosa* Zone. This conflict is caused by differences in the separation of *P. carpathica* and *E. nodosa*. The normal polarity zone J+ corresponds to SB-3n.1n. The reverse polarity interval K− corresponds to SB-3n.1r. These two polarity intervals in Silická Brezová belong to the uppermost *P. carpathica* Zone, and in the Erenkolu Mezarlik section to the lower *E. nodosa* Zone (for the explanation of this difference, see above). The normal polarity zone L+ corresponds to SB-3n.2n. In both Erenkolu Mezarlik and Silická Brezová the polarity zone is assigned to the *E. nodosa* Zone. The relatively thick reverse polarity zone M− corresponds to the very thin reverse polarity interval SB-3n.2r in Silická Brezová. The Lower Norian normal polarity zone N+ overlies a gap at Erenkolu Mezarlik, which comprises the entire *Metapolygnathus communisti–Epigondolella pseudodiebeli* Zone and a large part of the *E. primitia* Zone.

7.2. Bolücektası Tepe section, Antalya Nappes, Turkey

The Bolücektası Tepe section (Gallet et al., 1992, 1994) is a tectonically and sedimentologically complicated sequence of Hallstatt Limestones. There is a large gap between the Julian and the *Epigondolella nodosa* Zone of the upper part of Middle Tuvalian. Above the gap, the *E. nodosa* Zone, the *Metapolygnathus communisti* Zone, the *E. abneptis* Zone and the *E. triangularis–Norigondolella hallstattensis* Zone are exposed in Hallstatt Limestone facies. We have labelled the polarity zones BT-1n to BT-8n to facilitate discussion of the correlation with Silická Brezová (Fig. 14). Above a tectonic contact, allodapic limestones with numerous clasts represent the Alaunian (Middle Norian).

The Carnian–Norian boundary is not well marked at Bolücektası Tepe. *Norigondolella navicula* is absent (it is rare or missing throughout Neotethys). Only one sample yielded *Epigondolella* cf. *primitia* together with *Metapolygnathus communisti*, above which there is a thick conodont-free interval. As the age control in the Carnian–Norian boundary interval is poor, the correlation with Silická Brezová is problematic. The *E. nodosa* Zone of the Bolücektası Tepe section has predominantly normal polarity (BT-1n to lower BT-3n.2n) with three thin reverse polarity zones. This interval corresponds to SB-3n.1n to lower SB-3n.3n (Fig. 14). As discussed above, the uppermost *Paragondolella carpathica* Zone at Silická Brezová corresponds to the lower *E. nodosa* Zone in the papers by Gallet et al. Polarity zone SB-3n.1r lies in the uppermost *P. carpathica* Zone, whereas BT-1r lies, according to Gallet et al. (1994), in the lower *E. nodosa* Zone. In Gallet et al. (1994), the reverse polarity zone BT-3n.1r was assigned to the upper *E. nodosa* Zone, however, in Gallet et al. (2000) the 'Upper *Nodosus* range zone' of Gallet et al. (1994) was assigned to the *E. pseudodiebeli* Zone. Therefore, polarity zone BT-3n.1r appears to correspond to PM3r of Pizzo Mondello. The correlative polarity zone is missing at Silická Brezová because of an apparent gap in the lower *E. pseudodiebeli–M. communisti*. Zone. According to the new stratigraphic data by Gallet et al. (2000) for the lower BT-3n interval (including the short reverse BT-3n.1r level), the upper BT-3n corresponds to the upper SB-3n.3n that belongs to the *E. pseudodiebeli–M. communisti* Zone and the lower *E. primitia* Zone. As the FAD of *N. navicula* (used in the present paper as the base of the Norian) is in the uppermost part of SB-3n.3n, it should lie within the uppermost part of BT-3n.2n in the Bo-

lücektası Tepe section. This cannot be confirmed by the very sparse conodont data from this stratigraphic level in the Bolücektası Tepe section.

The uppermost range of *Metapolygnathus communisti* occurs in the upper part of polarity zone BT-3r. This species occurs at this level together with *Epigondolella*. cf. *primitia* and '*M. communisti* B'. It can be concluded that this level lies close the top of the *E. primitia* Zone, as *M. communisti* disappears within the upper *E. primitia* Zone (Orchard, 1991b). Above this level, there is an interval from which no conodonts where reported by Gallet et al. (1992), and then *E. abneptis* appears. According to these data, the *E. abneptis* Zone probably begins within the uppermost part of BT-3r, and this is in good agreement with Silická Brezová, where the *E. abneptis* Zone begins in the upper part of SB-3r. Polarity zones BT-4n to BT-7r can be correlated to SB-4n to SB-7r (Fig. 14), and the correlation is supported by conodont stratigraphy. However, as discussed in Section 5, the entire lower *E. triangularis* Zone of Gallet et al. (1992) corresponds to the upper *E. abneptis* Zone in the present paper (= upper *E. quadrata* Zone in Orchard, 1991a).

Above polarity zone BT-7r pronounced gaps are present in the Bolücektası Tepe section and, therefore, the correlation to other sections is problematic. The Alaunian is represented by allodapic limestones with numerous clasts, similar to the excluded middle part of the Silická Brezová trench section. However, the thick normal polarity zone in the upper *Epigondolella triangularis* Zone s.l. (BT-8n) is correlative to the normal polarity zones in Kavur Tepe (B+) and in Kavaalani (KV-13) (Gallet et al., 2000). The reverse polarity zone below BT-8n and above the gap at Bolücektası Tepe corresponds to the uppermost part of SB-8r at Silická Brezová. BT-10n and BT-10r correspond to SB-9n and the lower part of SB-9r, to D+ and lowermost E− of Kavur Tepe, and to KV-15 and lowermost KV-18 of Kavaalani. BT-10n corresponds to S-3n of Scheiblkogel. In several of these sections, a very thin reverse polarity zone, often indicated by only one sample, is present within uppermost BT-10n, in uppermost S-3n, and as reverse polarity zone KV-16 (Fig. 14).

7.3. Kavur Tepe section, Antalya Nappes, Turkey

The Kavur Tepe section (Gallet et al., 1993) lies in a klippe of highly condensed Hallstatt Limestones which cover the upper part of the *Epigondolella triangularis–Norigondolella hallstattensis* Zone of Lower Norian (Lacian) to the *Misikella hernsteini–Parvigondolella andrusovi* Zone of uppermost Sevatian. The Hallstatt Limestones are overlain by allodapic limestones with clasts that were not investigated by Gallet et al. (1993). To correlate Kavur Tepe with other sections, an original position in the Southern Hemisphere was assumed by Gallet et al. (1993). The Antalya Nappes were, however, derived from north of the Tauride High and were therefore situated in the Northern Hemisphere in Late Triassic time (Marcoux et al., 1989; Kozur, 2000; Gallet et al., 2000).

The Upper Lacian to Alaunian (except Upper Alaunian) part of the Kavur Tepe section corresponds to the unsampled interval in the Silická Brezová section. The Upper Lacian part can, both by conodont distribution and magnetic stratigraphy, be correlated with the upper *Epigondolella triangularis* Zone s.l. in the Bolücektası Tepe section (B+ = BT-8n) and the Kavaalani section (A− = upper KV-12, B+ = KV-13). In the Silická Brezová section, upper SB-8r corresponds to A− of the Kavur Tepe section.

The Upper Alaunian and Sevatian of Kavur Tepe can also be correlated with other sections. The Upper Alaunian is defined by Krystyn by a thick *Mockina slovakensis* Zone (*M. slovakensis* is named as *Epigondolella* n. sp. D, see Gallet et al., 2000) and a thinner *Parvigondolella vrielyncki* Zone (*P. vrielyncki* is named as *Epigondolella* n. sp. E, see Gallet et al., 2000). *P. vrielyncki* occurs in Silická Brezová exclusively in the lower part of the *Mockina bidentata* Zone, together with *M. bidentata* and *Monotis salinaria*. It is therefore a Sevatian form. However, *P. vrielyncki* is not as common as in the Neotethys, where it was also found in the lower *M. bidentata* Zone. The holotype of *M. slovakensis* is from the Norian–Rhaetian boundary level. In the northern Tethys this species is common in Sevatian restricted basin facies (Kovács and Nagy, 1989; Catalano et al.,

1990), but rare in Sevatian open sea facies. We have not yet found *M. slovakensis* below the FAD of the Sevatian *M. bidentata*, however *M. bidentata* may be absent in samples with *M. slovakensis* for facies reasons. This does not mean that *M. slovakensis* is necessarily absent below the FAD of *M. bidentata*. In the Neotethys of Sicily and southern Italy (Lagonegro Basin), *M. slovakensis* is very common in open sea Sevatian deposits. It is rare in the northern Tethys, and may begin in the Upper Alaunian (Gullo, 1996). In Timor (Krystyn, unpublished data), it occurs only in the uppermost Alaunian. However, our unpublished data from Turkey show a similar range as in the European Tethys (uppermost Alaunian–Sevatian). These data concerning the range of *M. slovakensis* and *P. vrielyncki* show that the base of the Sevatian (as defined in Silická Brezová) lies in Kavur Tepe within the lower part of Alaunian 3 sensu Gallet et al. (1993).

The normal polarity zone D+ at Kavur Tepe corresponds to SB-9n at Silická Brezová, and with Upper Alaunian conodont fauna in both sections. Reverse polarity zone E− at Kavur Tepe can be correlated with SB-9r (Fig. 14). According to the remarks made above, the base of the Sevatian is not within the upper third of E−, but at the top of the lower third of this reverse polarity zone. The normal polarity zone F+ corresponds to SB-10n. Both are within the *E. bidentata* Zone. The reverse polarity zone G− corresponds to SB-10r. The normal polarity H+ corresponds to SB-11n. The reverse polarity zone I− corresponds to the lower part of SB-11r.

The reverse polarity zone G− is situated within the upper *Mockina bidentata* Zone in Kavur Tepe, whereas the equivalent S-4r of the Scheiblkogel section lies at the top of the *M. bidentata* Zone, and SB-10r in Silická Brezová is situated within the lowermost *Misikella hernsteini–Parvigondolella andrusovi* Zone. This slightly different position implies a different onset of *M. hernsteini* in these three sections. Gallet et al. (1993, 2000) marked the base of their Sevatian 2 with the FAD of *M. hernsteini*. However, this datum is poorly defined biostratigraphically. *M. longidentata*, the forerunner of *M. hernsteini*, is known from the uppermost Carnian to Middle Norian. *M. hernsteini* is known from Upper Sevatian to Lower Rhaetian. The FAD of *M. hernsteini* lies anywhere between the top of the Alaunian and the Upper Sevatian. We use the *M. hernsteini–P. andrusovi* Zone and define the base of this zone by the dominance of *P. andrusovi* vs. *M. bidentata*, the FAD of *Parvigondolella lata* and the FAD of *M. hernsteini*. *P. lata* begins at the level where *P. andrusovi* becomes dominant relative to *M. bidentata*. *P. andrusovi* is similar to juvenile stages of *M. bidentata*, but has a distinct blade behind the cusp. *P. lata* evolved from *P. andrusovi* and its FAD is therefore rather well fixed in the Upper Sevatian. The FAD of *M. hernsteini* in the different sections may be at the same level or above the FAD of *P. lata*, indicating different positions of the appearance of *M. hernsteini* in different sections. At Silická Brezová the appearance of *M. hernsteini* is very early as it coincides closely with the FAD of *P. lata*. Consequently, the reverse polarity zone SB-10r lies within the lowermost *M. hernsteini–P. andrusovi* Zone.

The thickness of normal and reverse polarity zones is rather different at Silická Brezová and Kavur Tepe. This indicates variable deposition rates in the Sevatian of Kavur Tepe because this difference is not so apparent when Silická Brezová and Scheiblkogel are compared.

7.4. Scheiblkogel section, Austria

The nearly complete Middle and Upper Norian at Scheiblkogel consists of 23 m of condensed Hallstatt Limestones that are well dated with conodonts and ammonoids by Krystyn in Gallet et al. (1996). According to Gallet et al. (2000), there is a gap between the Alaunian and Sevatian at Scheiblkogel. Most of the Upper Sevatian of the Scheiblkogel section has not yielded conodonts. Close to the top of the section the ammonoid *Cochloceras* was reported by Gallet et al. (1996). Kozur (1996) found *Misikella posthernsteini*, the Rhaetian conodont guideform, within red Hallstatt Limestones of the *Cochloceras suessi* Zone. As the uppermost two meters of the Scheiblkogel section are gray Hangendgraukalk, a Rhaetian age for the level with *Cochloceras* is probable. There is no consensus on the definition of the

Norian–Rhaetian boundary. Viable candidates for the base of the Rhaetian are: the FAD of *M. posthernsteini* in the Tethys and western Panthalassa, the base of the *Cochloceras suessi* Zone in the Tethys and the base of the *Cochloceras amoenum* Zone in western North America. These events are more or less contemporaneous and correlate with the FAD of '*Mockina*' *mosheri* (Kozur, 1996; Orchard and Tozer, 1997) and probably also to the FAD of *M. posthernsteini*.

The polarity zones at Scheiblkogel are labelled S-1r to S-6n (Fig. 14). The Upper Alaunian normal polarity zone S-3n in the Scheiblkogel section can be correlated with the normal polarity zone SB-9n, and both have Alaunian conodont faunas. S-3r corresponds to the Sevatian upper 2/3 of SB-9r. The Upper Alaunian lower third of SB-9r is absent in the Scheiblkogel section, confirming the presence of a short gap between the Alaunian and Sevatian in the Scheiblkogel section as already assumed by Gallet et al. (1996). The relatively thick normal polarity zone S-4n corresponds to the thick normal polarity zone SB-10n at Silická Brezová. Both lie within the *E. bidentata* Zone. The thinner polarity zone S-4r can be correlated with SB-10r. For reasons discussed in the Bolücektası Tepe section, S-4r is assigned to the uppermost *E. bidentata* Zone, whereas the contemporaneous SB-10r belongs to the lowermost *Misikella hernsteini–Parvigondolella andrusovi* Zone. The somewhat thicker S-5n and the likewise somewhat thicker SB-11n correlate with each other and are both assigned to the *M. hernsteini–P. andrusovi* Zone (Fig. 14; Gallet et al., 1996). Polarity zone SB-11r is relatively thick at Silická Brezová, indicating an increase in sedimentation rate that is denoted by several layers of calcarenites between the Hallstatt Limestones. The upper part of SB-11r is cut away by a fault in the Silická Brezová section. As is generally the case in the Silica Nappe, the Upper Norian sections end at the boundary between the Hallstatt Limestones and the soft marls of the Zlambach Beds. Because of this facies change this boundary is a preferred thrust plane in the Silica Nappe. Where the Zlambach Marls are preserved, they are always of Rhaetian age. Thus, the top of the sampled Silická Brezová trench section is at, or very close to, the Norian–Rhaetian boundary (as indicated also by advanced *M. hernsteini*) which lies seemingly within the reverse polarity zone SB-11r. This is in good agreement with the Scheiblkogel section, if we define the base of the Rhaetian with the FAD of *Cochloceras* (and the probably contemporaneous FAD of *Misikella posthernsteini*). *Cochloceras* appears in the middle part of S-5r. Thus, SB-11r corresponds only to the lower part of S-5r.

7.5. Kavaalani section of Antalya Nappes, Turkey

The Kavaalani section in the Antalya nappes of southern Turkey consists of a condensed sequence of 55 m of Hallstatt Limestones which cover the Upper Tuvalian to Lower Sevatian interval (Gallet et al., 2000). The section is well dated by conodonts (Krystyn in Gallet et al., 2000). The following correlations can be established. The normal polarity zone KV-1 corresponds to SB-3n.2n; both lie in the *Epigondolella nodosa* Zone. The reverse polarity zone KV-2 corresponds to SB-3n.2r; both are also situated in the *E. nodosa* Zone. The normal polarity zone KV-3 corresponds to the lower part of SB-3n.3n. The short reverse polarity zone (KV-4), immediately below a gap, corresponds to the short reverse polarity interval within the *Metapolygnathus communisti-E. pseudodiebeli* Zone which is not present at Silická Brezová. At the gap between the Tuvalian and Lacian in the Kavaalani section, the upper part of SB-3n.3n and the entire SB-3r (upper part of *E. pseudodiebeli–M. communisti* Zone and *E. primitia* Zone) is absent. The normal polarity zone above the gap (KV-5) corresponds to SB-4n. This would mean, however, that the '*M. communisti* B' Zone in Kavaalani corresponds to the lower *E. abneptis* Zone at Silická Brezová. The '*M. communisti* B' Zone is Early Norian in age, if we use the FAD of *Norigondolella navicula* for its definition, but the exact range of the '*M. communisti* B' Zone within the Early Norian is unknown. Most probably, it corresponds to the upper *E. primitia* Zone and lower *E. abneptis* Zone. The Lacian interval from the reverse polarity zone KV-6 to the normal polarity KV-11 can be correlated with the Silická Brezová and Bolücektası Tepe sections (Fig. 14) where it

corresponds to the *E. abneptis* Zone (= *E. quadrata* Zone sensu Orchard, 1991a; = *E. abneptis* A Zone and lower *E. triangularis* Zone sensu Gallet et al., 2000).

The thick reverse polarity zone KV-12 corresponds to the interval from SB-7r to SB-8r. As the short normal polarity zone SB-8n was not found in the Kavaalani section, the base of the *Epigondolella triangularis–Norigondolella hallstattensis* Zone lies in the middle part of the reverse polarity zone KV-12. The uppermost Lower Norian normal polarity zone KV-13 corresponds to the upper *E. triangularis–N. hallstattensis* Zone s.l. (including *E. spatulata* Zone) and correlates to the not investigated part in the Silická Brezová trench section. KV-13 is, however, easy to correlate with BT-8n from the Bolücektası Tepe section and B+ of the Kavur Tepe section.

The Middle Norian is very incomplete in the Kavaalani section, but its basal and upper parts are, as in several other sections, well exposed and not sedimentologically complicated. The Lacian–Alaunian boundary is situated within the uppermost part of a long normal interval (KV-13) which starts in the upper *Epigondolella triangularis* Zone s.l. A short reverse interval (KV-14) follows, and a little above this interval the largest part of the Lower Alaunian and the entire Middle Alaunian is missing in a stratigraphic gap. The magnetostratigraphic succession across the Lacian–Alaunian boundary is similar to that at Kavur Tepe, where, however, more of the Lower Alaunian *Mockina medionorica–M. matthewi* Zone is preserved.

The Upper Alaunian begins above the Middle Alaunian gap with a normal polarity interval (KV-15), which can be correlated with SB-9n of Silická Brezová, S-3n of Scheiblkogel, D+ of Kavur Tepe, and BT-10n of Bolücektası Tepe. The overlying reverse interval (KV-18) can be correlated with SB-9r of Silická Brezová and E− of Kavur Tepe. Its lower (uppermost Alaunian) part correlates to BT-10r of Bolücektası Tepe and its upper (lowermost Sevatian) part with S-3r of Scheiblkogel (Fig. 14). The Alaunian–Sevatian boundary lies within the reverse interval KV-18. The normal polarity interval KV-19 of the *E. bidentata* Zone, in which the Kavaalani section ends, corresponds to the lower part of SB-10n of Silická Brezová, lower part of S-4n of Scheiblkogel, and lower part of F+ of Kavur Tepe, all situated within the *Mockina bidentata* Zone.

7.6. Correlation with the Newark Basin

In the Newark Basin, almost 5 km of Upper Carnian to Rhaetian continental sediments have provided a magnetostratigraphic template for the Late Triassic geomagnetic polarity time scale (GPTS) with a robust astrochronology based on depositional cycles (Kent et al., 1995; Kent and Olsen, 1999, 2000). Adopting a Southern Hemisphere origin for Kavur Tepe, Kent et al. (1995) proposed a correlation of the Kavur Tepe section to the E14–E19n interval in the Newark Basin (Fig. 14). These authors were unable to find a satisfactory correlation of the Bolücektası Tepe section to Newark. As an illustration of the continuing correlation dilemma, Muttoni et al. (2001) correlated the Kavur Tepe magnetostratigraphy, both for a Southern Hemisphere and Northern Hemisphere origin, to the E18–E22 interval at Newark. In so doing, they appear to have correlated well-dated Lower to Upper Norian marine strata with Rhaetian continental strata of the Newark Basin. Muttoni et al. (2001) correlated the polarity zones of Pizzo Mondello (PM1–6) (Fig. 14), which belong to the Middle Tuvalian *Epigondolella nodosa* Zone–Lower Norian *E. abneptis* Zone, to the E13–E17 interval at Newark. This interval at Newark is, however, undoubtedly Norian and ranges into the uppermost Norian.

Other Upper Triassic magnetostratigraphies from the Chinle Group (e.g. Steiner and Lucas, 2000), North Sea (Hounslow et al., 1995) and South England (Briden and Daniels, 1999) have been correlated to the E12–E18 (Upper Lacian to Lower Rhaetian) interval at Newark. Yet again, the lack of biostratigraphic ties, the indistinctive polarity zone pattern, and the brevity of the sampled sections makes the stratigraphic correlations equivocal.

From polarity zone E8 to E12 in Newark (Fig. 14), the polarity sequence is characterized by relatively thin normal polarity zones and relatively thick reverse polarity zones. The logical correla-

tion is to polarity zones SB-4 to SB-8 at Silická Brezová. Polarity zones E15 and E16 are dominated by normal polarity, as are SB-9 and SB-10 at Silická Brezová. Polarity zone E15 corresponds to SB-9, however, the thin normal polarity zone within E15r is absent in SB-9r. E13 and E14 correspond to the Middle Norian that was not investigated at Silická Brezová. Polarity zones E5–E7 of the Newark Basin are part of SB-3 in the Silická Brezová section. E5 consists of two normal and two reverse polarity intervals, of which the lower normal polarity interval is the thickest. The two reverse polarity zones within E5 correspond to SB-3n.1r and SB 3n.2r. E6 corresponds to the lower part of SB-3n.3n, where the reverse polarity zone is apparently missing at Silická Brezová within the *Metapolygnathus communisti–Epigondolella pseudodiebeli* Zone. This reverse polarity zone is, however, present in several other sections and is best dated at Pizzo Mondello (PM3r, Muttoni et al., 2001). This reverse polarity interval and the lower part of the normal polarity interval SB-3n.3n corresponds to E6. The upper part of SB3n.3n, in the upper *M. communisti–E. pseudodiebeli* Zone and in the lower *E. primitia* Zone, corresponds to E7n at Newark (Fig. 14). The following thinner reverse polarity zone SB-3r in the upper *E. primitia* Zone and at the very base of the *E. abneptis* Zone (Fig. 14) corresponds to E7r. Therefore, the Carnian–Norian boundary lies close to the top of the normal polarity zone E7n. This is in the Upper Stockton Formation close to the base of the Raven Rock Member.

Polarity zones E3–E7 in the Newark Basin, derived from the Princeton long core (Kent et al., 1995), are more equivocal than the rest of the generally pristine Newark magnetostratigraphic record, and there is some evidence for a stratigraphic hiatus which has had the effect of thinning polarity zone E7r (Olsen, pers. commun., 2002). The correlation of this interval to the SB-1 to SB-3 interval in Silická Brezová is problematic and implies highly variable sedimentation rates at Silická Brezová (Fig. 15). The bioclastic limestones in the Lower Trench at Silická Brezová (Fig. 2) are at the transition facies from the Wetterstein Limestones to the Hallstatt Limestones and would be expected to have elevated sedimentation rates. Above this facies transition, the sedimentation rates at Silická Brezová are in the 2–14 m/Myr range (Fig. 15). Sedimentation rates within SB3n.2r and SB3n.3n are the lowest in the section, at 2.4 m/Myr.

As discussed above in reference to the Scheiblkogel section, the Norian–Rhaetian boundary, as defined by the FAD of *Cochloceras*, lies within the middle part of S-5r corresponding to the top of SB-11r (end of the outcrop at the top of the Norian), and to the middle part of E17r at Newark. Thus, the base of the Rhaetian lies close to the level assumed by Kent and Olsen (2000) for this stage boundary at the base of E18.

8. The Rhaetian and the poorly-exposed/brecciated interval at Silická Brezová

At Silická Brezová the sedimentologically and tectonically complicated uppermost Lacian to Middle Alaunian part of the trench section with brecciated limestones and fissure fillings was not investigated for magnetic stratigraphy. In the quarry sections the outcrops terminate in the middle *Epigondolella triangularis* Zone (Fig. 2). At Silická Brezová, no magnetostratigraphic data are available for the upper *E. triangularis* Zone up to the Middle Alaunian. The trench section ends at a fault at the Norian–Rhaetian boundary (thrust-plane at the boundary between Hallstatt Limestone and Zlambach Marls). For this reason, we also have no magnetostratigraphic data from the Rhaetian.

Unfortunately, the Alaunian (except the Upper Alaunian) is sedimentologically very complicated not only at Silická Brezová but also in the Turkish sections and at Scheiblkogel. SB-8 of Silická Brezová can be correlated to E12 of the Upper Lockatong Formation in the Newark Basin. The long normal interval BT-8n of Bolücektası Tepe, B+ of Kavur Tepe and KV-13 of Kavaalani can be correlated with E13n (Fig. 14). This long normal interval is well dated by conodonts as part of the upper *Epigondolella triangularis* Zone s.l. (including the *E. spatulata* Zone sensu Gallet et al., 2000). Both in Kavur Tepe and in Kavaalani, the base of the Alaunian is exposed and well dated by

conodonts within the uppermost part of this long normal interval. Therefore, the base of the Alaunian in the Newark Basin is within the uppermost part of E13n. The Alaunian–Sevatian boundary at Silická Brezová lies within SB-9r. This boundary is easy to correlate with other marine sections (Kavur Tepe, Kavaalani, Scheiblkogel, see Fig. 14), but also with the Newark Basin, where it is situated within E15r. The Alaunian interval of the Newark Basin is therefore correlated to the interval between the uppermost part of E13n to the lower part of E15r. Bolücektası Tepe, Kavur Tepe and Kavaalani are too fragmentary in the Alaunian to yield any reliable marine standard for this time interval. The gaps within the Alaunian, indicated by Gallet et al. (2000), are too long to yield reliable data for subdivision of the marine Alaunian (Fig. 14). However, the situation is different at Scheiblkogel where three gaps are indicated within the Alaunian, but they are seemingly so short that despite of these gaps the basic magnetostratigraphic pattern of the Alaunian, a R–N–R–N sequence of polarity zones, is preserved. Unfortunately, the lower boundary of the Alaunian is not exposed, but it is seemingly close to the exposed base of the section, where one single measurement of normal polarity is present which may belong to the top of the long normal interval, equivalent to E13n. At the Alaunian–Sevatian boundary, there is a gap, where the topmost Alaunian reverse zone (equivalent to the lower SB-9r of Silická Brezová, BT-10r of Bolücektası Tepe, lower E− of Kavur Tepe, lower KV-18 of Kavaalani and lower E15r of the Newark Basin) is missing (Fig. 14). Nevertheless, more of the Alaunian is present in Scheiblkogel than in any other investigated marine section. S-1r of Scheiblkogel corresponds to E13r of the Newark Basin, S-2n to E14n, S-2r to E14r and S-3n to E15n.

The base of the Rhaetian, defined with the FAD of *Cochloceras* and '*Mockina*' *mosheri* (and the more or less contemporaneous FAD of *M. posthernsteini*) is situated in the middle part of S-5r at Scheiblkogel, which corresponds to the top of SB-11r at Silická Brezová. This level corresponds to the middle part of E17r in the Newark Basin. As the base of the Jurassic is well defined in the Newark Basin (base of E24), the Newark polarity zonation for the Rhaetian (upper E17r to the top of E23) can be taken as magnetostratigraphic standard for the Rhaetian. The correlation with the biostratigraphic subdivision of the marine Rhaetian is not yet possible because no marine Rhaetian sections have been magnetostratigraphically investigated.

9. Implications for the Newark Basin stratigraphy

Assuming continuous sedimentation for the Newark section, the polarity zone pattern fit of Silická Brezová to Newark (Fig. 14) indicates a lower position for the base of the Norian in the Newark Basin than all previous biostratigraphic correlations. The Carnian–Norian boundary apparently lies in the lower third of the New Oxford–Lockatong palynofloral zone that has been assigned to the Upper Carnian (Cornet, 1993; Kent and Olsen, 2000). This position for the Carnian–Norian boundary corresponds to the lower third of the Conewagian land vertebrate faunachron (LVF) dated, on the basis of the palynological correlations, as Late Carnian (Huber and Lucas, 1996). Our correlation implies that the New Oxford–Lockatong palynofloral zone and also the Conewagian LVF are incorrectly correlated with the marine stratigraphy. The Lockatong Formation is dated as Late Carnian by sporomorphs, megaplants and vertebrates (Cornet, 1993; Huber and Lucas, 1996; Kent and Olsen, 2000), but in reality, the Late Carnian age of the vertebrates is based on the sporomorph correlation and not on direct vertebrate correlation.

The revised magnetostratigraphic correlations imply that the paleomagnetically investigated part of the Stockton Formation does not reach the base of Carnian, as assumed by Kent and Olsen (2000). The base of the Stockton Formation appears to extend to just above the base of the Tuvalian at 231 Ma (Fig. 14). Huber et al. (1993) came to a similar conclusion based on biostratigraphic analyses. These authors correlated the base of the Stockton Formation to the Lower Tuvalian. The Ladinian–Carnian boundary is therefore significantly older than 231 Ma. If we

assume a 1–1.5-Myr duration for each Cordevolian and Julian ammonoid zone, the Ladinian–Carnian boundary would be around 237 Ma, consistent with the age for the upper Ladinian *Archelaus* Zone of 238 Ma from Mundil et al. (1996).

The regional Sanfordian LVF of the Lower Stockton Formation in the Newark Basin corresponds to the global Otischalkian LVF (Lucas, 1998), to which belong the tetrapod faunas of the Kieselsandstein and Blasensandstein of the Germanic Basin. Lucas and Heckert (2001) assigned the Blasensandstein to the Lower Adamanian. These units belong to the Tuvalian, but not to the latest Tuvalian (Kozur, 1993). This age is confirmed by the discovery of *Paleorhinus*, typical of the Otischalkian to Lower Adamanian LVF, in the Tuvalian of Austria. The regional Neshanician LVF of the Lower Passaic Formation of the Newark Basin belongs to the lower part of the global Revueltian LVF. This part of the Revueltian is well dated as Upper Alaunian in the marine beds of Italy. This is consistent with our paleomagnetic correlation of the Neshanician LVF with the uppermost Lacian and Alaunian. The oldest fauna of the Revueltian LVF is that of the Lower Stubensandstein in the Germanic Basin. According to its conchostracan fauna it belongs to the upper part of Lower Norian (Upper Lacian) or Lower Alaunian.

The regional Conewagian LVF, between the top of the well-dated Sanfordian and the base of the well-dated Neshanician, spans the interval from uppermost Tuvalian to Lower Lacian. According to Lucas (1998), the regional Conewagian LVF of the Newark Basin corresponds to the global Adamanian LVF. Unfortunately, there is no direct correlation between the Adamanian LVF and marine biostratigraphy, except for the Lower Adamanian that corresponds to uppermost Tuvalian. According to Lucas (1998), the Adamanian LVF corresponds to the uppermost Carnian but he also pointed out that it is not clear whether the overlying Revueltian begins at the base of the Norian. According to our paleomagnetic correlation with Silická Brezová only the basal part of the Conewagian (Adamanian) LVF is latest Tuvalian in age, but the largest part is Lower Norian in age. According to Lucas (1998), the latest Carnian age of the Adamanian LVF is based on palynostratigraphy, sequence stratigraphy and magnetostratigraphy. The Conewagian LVF was assigned to the New Oxford–Lockatong assemblage that was, in turn, assigned to a Late Carnian age. On this basis, the Upper Carnian was assigned to the Lockatong Formation of Newark Basin. The vertebrates of the Adamanian LVF are either restricted to this faunachron, like *Rutiodon* and *Stagonolepis*, or begin in this faunachron and range up into undisputed Norian or younger strata (*Desmatosuchus*), or they are long-ranging forms without particular stratigraphic significance. The typical Tuvalian *Paleorhinus* which was also found in marine Tuvalian beds (Lucas, 1998), is not present in the Adamanian LVF, except in the lowermost Adamanian, where it occurs together with typically Adamanian *Stagonolepis*.

Based on this discussion, the palynology plays the decisive role in correlating the Newark strata to the Carnian–Norian boundary. The New Oxford–Lockatong palynoflora involves taxa that range up from undoubtedly Tuvalian. In the New Oxford–Lockatong sporomorph association, that has the same range as the Conewagian LVF, the Norian guideform *Camerosporites verrucosus* occurs and becomes increasingly abundant within the interval. This was explained by Cornet (1993) in terms of an earlier occurrence of the Norian guideform in the Late Tuvalian of the equatorial (Newark) region. This is one possible explanation. However, Carnian forms ranging into the Early Norian in the equatorial (Newark) region can also explain it. This is even more probable because *C. verrucosus* occurs in the Chinle Group only in the undisputed Norian part (Cornet, 1993). Also, *Kyrtomisporis laevigatus* begins in the Chinle Group only in the Norian part, and in the Newark Basin in the New Oxford–Lockatong sporomorph association. Thus, a latest Tuvalian age of the New Oxford–Lockatong sporomorph association is only a possibility, but not independently proven. Sporomorphs do not exclude a Lower Norian age for these rocks. The very rich conchostracan fauna of the Lockatong Formation, the only conchostracan fauna of the Newark Basin that has been described in some

detail (Bock, 1953a,b), is not yet known outside North America. It is younger than the Upper Tuvalian *Palaeolimnadia nakazawai* Zone and older than the Upper Lacian to Lower Alaunian *Shipingia dorsorecta* Zone. The *Shipingia dorsorecta* Zone occurs in the upper part of the Upper Variegated Marls and in the Lower Stubensandstein of the southern Germanic Basin, and in the Newark Supergroup in equivalents of the Lower Passaic Formation in the Culpeper Basin. The conchostracans indicate, therefore, a latest Tuvalian to Early Norian age for the Adamanian LVF. The Lockatong Formation and Upper Stockton Formations appear to belong to the Lower Norian, confirming our magnetostratigraphic correlation.

10. Conclusions

The HBT magnetization component at Silická Brezová has yielded a magnetic polarity stratigraphy that can be correlated with the magnetostratigraphy of Upper Carnian and Norian sections from Turkey and Austria published by Gallet et al. (1992, 1993, 1994, 1996, 2000). The correlations require a Northern Hemisphere (rather than Southern Hemisphere) origin for Kavur Tepe, which is in agreement with the geological data and is also accepted by Gallet et al. (2000). A re-evaluation of the conodont stratigraphies leads to some important conclusions that may reduce the confusion presently surrounding Upper Triassic conodont biostratigraphy. The conclusions include the change of the boundary between the *Epigondolella abneptis* and *E. triangularis–Norigondolella hallstattensis* zones, and the assignment of the *E. spatulata* Zone to the uppermost *E. triangularis* Zone. This results in a consistent *E. triangularis–N. hallstattensis* Zone in North America and in the Tethys. The definition of the *E. spatulata* Zone by Gallet et al. (2000) may provide a useful subdivision of the *E. triangularis–N. hallstattensis* Zone. Other conclusions include: (1) the assignment of the upper part of the *Mockina slovakensis* (*Epigondolella* n. sp. D sensu Gallet et al., 1992, 1993, 1996, 2000, species assignment after Gallet et al., 2000) and of the *Parvigondolella vrielyncki* fauna (*Epigondolella* sp. E, species assignment after Gallet et al., 2000) to the Lower Sevatian *M. bidentata* Zone, and (2) the assignment of the Upper Sevatian 2 with *Cochloceras* (but without conodonts) to the Rhaetian.

The correlation of the different marine magnetostratigraphic sections has allowed us to infer a composite magnetostratigraphic sequence for the marine Tuvalian to lowermost Rhaetian of the Tethys which can be correlated to the Newark Basin polarity record (Kent et al., 1995; Kent and Olsen, 1999, 2000). The paleomagnetically investigated sections of the Stockton Formation in the Newark Basin have their base within the Lower Tuvalian, somewhat above the base of the Tuvalian. This is in agreement with the biostratigraphic correlations by Huber et al. (1993). The Carnian–Norian boundary defined by the FAD of *Norigondolella navicula* at the base of the upper *Epigondolella primitia* Zone lies in the Upper Stockton Formation of the Newark Basin, immediately below the Raven Rock Member. This level is within the lower part of the New Oxford–Lockatong palynological assemblage and within the lower part of the Adamanian and equivalent Conewagian LVF. Previously, these palynological and tetrapod units of the Upper Stockton Formation and Lockatong Formation were assigned to the latest Tuvalian. However, this traditional age assignment relies exclusively on palynological data (and the associated macrofloral data). Except for the lowermost Adamanian (Conewagian), the land vertebrates are represented either by taxa restricted to the Conewagian LVF, or by long-ranging taxa that occur also in the underlying well-correlated Tuvalian (Sanfordian LVF) and overlying well-correlated Norian (Neshanician LVF). The most important vertebrates of Conewagian LVF, like *Rutiodon*, are restricted to this interval and cannot be directly correlated with marine stratigraphy. They are younger than the *Paleorhinus* (without *Stagonolepis*) assemblage of the Otischalkian LVF, that can be directly correlated (using vertebrates) with the marine Tuvalian or to faunas in the Germanic Basin that are correlated with the Tuvalian. Direct correlations of the Neshanician LVF vertebrate faunas with marine beds have shown a Late Alaunian age.

The oldest Revueltian faunas (Neshanician LVF corresponds to the lower and middle Revueltian) are known from the Germanic Lower Stubensandstein. Here the tetrapod-bearing levels contain Conchostraca of the upper Lacian to lower Alaunian *Shipingia dorsorecta* Zone that is also present in the Culpeper Basin in equivalents of the Lower Passaic Formation (Kozur and Weems, in preparation). The next lower conchostracan horizon of the Germanic Basin, the Coburg Sandstein, has a latest Carnian conchostracan fauna. Immediately below this conchostracan horizon, in the Blasensandstein at Ebrach, is the uppermost occurrence of the Tuvalian guideform *Paleorhinus*. At the same level is the FAD of *Stagonolepis*, a guideform of the Adamanian. This horizon with co-occurrence of the Otischalkian and Adamanian guideforms is also known from Arizona and defines the uppermost Tuvalian and the lowermost Adamanian (Lucas and Heckert, 2001). According to our magnetostratigraphic correlations, and also according to the vertebrate fauna with *Paleorhinus* and *Stagonolepis*, the lowermost Adamanian LVF (=lowermost Conewagian) corresponds to the uppermost Tuvalian. The next higher well-correlated Lower Revueltan tetrapod fauna corresponds to the uppermost Lacian and Middle Norian. A Lower Lacian age of the Raven Rock Member of the uppermost Stockton Formation and the Lockatong Formation is implied. The New Oxford–Lockatong palynological assemblage contains, however, Carnian forms together with the Norian guide form *Camerosporites verrucosus*. This was explained by an earlier FAD of Norian guide forms in the equatorial Newark Basin, and, on this basis, a latest Tuvalian age was established for the New Oxford–Lockatong palynological assemblage. The distribution can also be explained by a later disappearance of Carnian sporomorphs within the Lower Norian of the equatorial belt. This is consistent with the presence of *Camerosporites verrucosus* in the Norian beds of the Chinle Group.

The Neshanician LVF corresponds, according to our magnetostratigraphic correlation, to the uppermost Lacian, Alaunian and lowermost Sevatian. This is in good agreement with the direct correlation of tetrapods from the Neshanician LVF (Lower–Middle Revueltian) with marine beds of Late Alaunian age (Lucas, 1998). The base of the Rhaetian is in the middle part of E17r, very close to the previously assumed base of the Rhaetian at the base of, or within, E18 (Kent and Olsen, 2000).

The combination of Newark astrochronology with the previous designation of stage boundaries (Kent and Olsen, 2000) yielded the following stage durations: Rhaetian, 6 Myr; Norian, 9.5 Myr; and Tuvalian, 15.5 Myr. This implied a duration of ~21.5 Myr for the Carnian (including 6 Myr for Cordevolian and Julian). Adopting the 200-Ma age for the Triassic–Jurassic boundary (Pálfy et al., 2000, 2002), the astronomically tuned GPTS of Kent and Olsen (1999), and our revised correlation of the marine stage boundaries with the Newark succession, the following durations for the Upper Triassic stages are estimated: Rhaetian 207–200 Ma (7 Myr), Norian 207–226 Ma (19 Myr) and Carnian 226–237 Ma (11 Myr, including 5 Myr for Tuvalian and 6 Myr for Cordevolian+Julian). This yields a duration for the Norian that is 2.7 times that of the Rhaetian, and a Norian duration 1.72 times that of the Carnian.

Acknowledgements

We dedicate this work to our friend and colleague Rudi Mock who died in August, 1996. He was a superb geologist and alpine climber, and was an inspiration to those of us who were fortunate enough to know him. He was the instigator of this project, organized the trenching of the section at Silická Brezová and took part in our first two field campaigns. We gratefully acknowledge assistance in the field from Giovanni Muttoni and Dennis Kent, and helpful discussions with Giovanni Muttoni, Dennis Kent, Paul Olsen, Alda Nicora, Leopold Krystyn, and Spencer Lucas. Michael Orchard and Dennis Kent provided useful comments in reviews of the manuscript. The US National Science Foundation (Grant EAR-9417895) supported this research. Contribution to IGCP467.

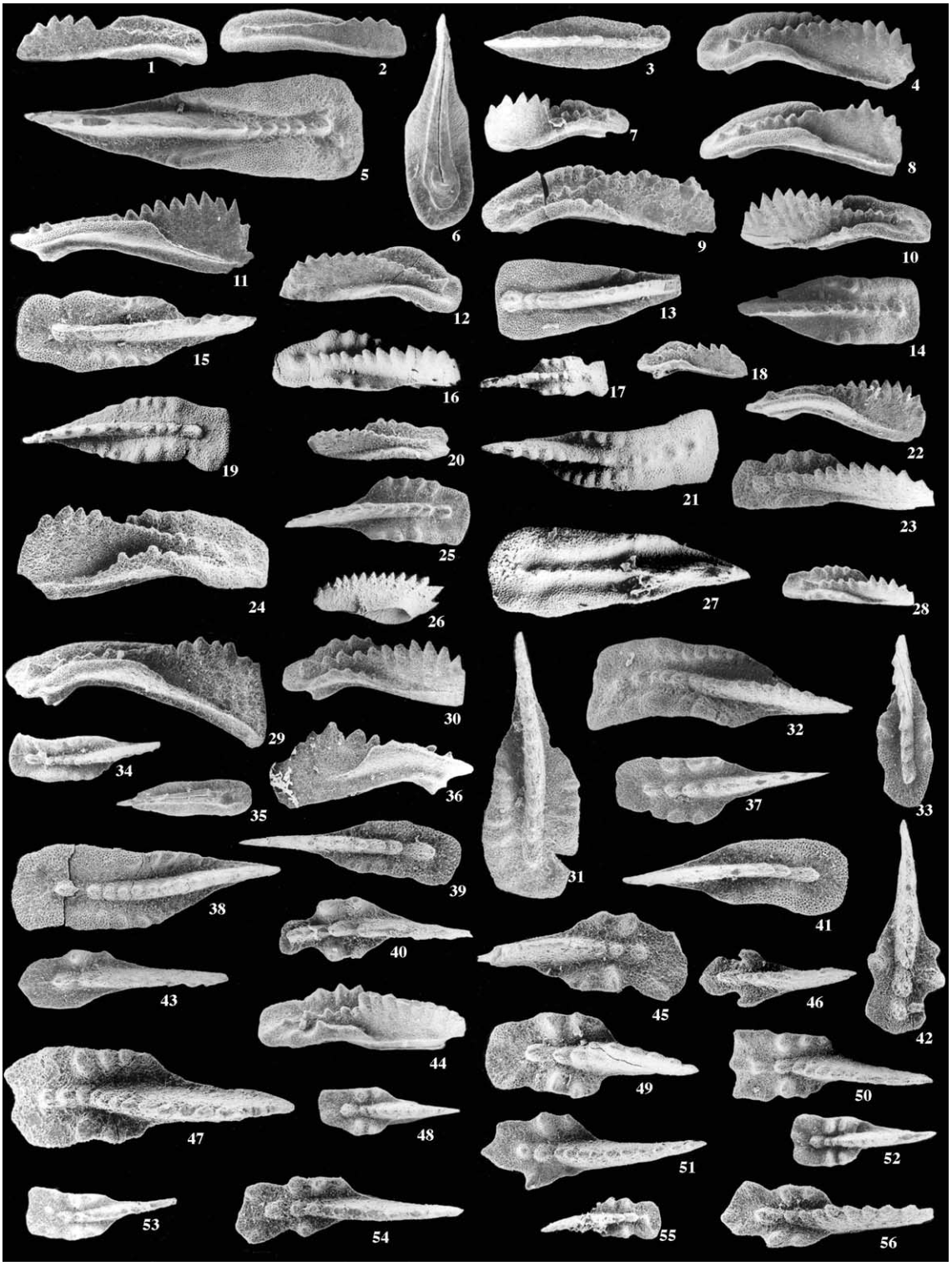
1
2
3
4
5
6
7
8
9
10
11
12
13
14
15
16
17
18
19
20
21
22
23
24
25
26
27
28
29
30
31
32
33
34
35
36
37
38
39
40
41
42
43
44
45
46
47
48
49
50
51
52
53
54
55
56

Fig. A1.

Fig. A1. All illustrated specimens are from the trench section near Silická Brezová. The meter levels indicate m above the base of the trench section.

1. *Paragondolella polygnathiformis noah* (Hayashi), oblique lateral–upper view, ×50, *P. polygnathiformis noah* Zone, Lower Tuvalian, 0.2 m, rep.-No. 31-3-98/I-2.
2. *Paragondolella postinclinata* n. sp., holotype, oblique lateral–upper view, ×50, *P. polygnathiformis noah* Zone, Lower Tuvalian, 0.2 m, rep.-No. 31-3-98/I-1.
3. *Paragondolella praelindae* n. sp., holotype, upper view, ×50, *P. polygnathiformis noah* Zone, Lower Tuvalian, 1.1 m, rep.-No. 9-2-99/I-45.
4. *Paragondolella carpathica* (Mock), oblique lateral–upper view, ×50, *P. carpathica* Zone, Middle Tuvalian, 4.0 m, rep.-No. 31-3-98/I-6.
5. *Paragondolella carpathica* (Mock), upper view, ×40, *P. carpathica* Zone, Middle Tuvalian, 4.0 m, rep.-No. 31-3-98/I-8.
6. *Paragondolella polygnathiformis noah (*Hayashi), lower view, ×50, *P. carpathica* Zone, Middle Tuvalian, 9 m, rep.-No. 31-3-98/I-10.
7. *Paragondolella carpathica* (Mock), juvenile specimen, oblique lateral view, ×50, *P. carpathica* Zone, Middle Tuvalian, 2.0 m, rep.-No. 9-2-99/I-49.
8. *Paragondolella polygnathiformis noah (*Hayashi), oblique lateral view, ×50, *P. carpathica* Zone, Middle Tuvalian, 9.0 m, rep.-No. 31-3-98/I-9.
9. *Paragondolella carpathica* (Mock), advanced specimen, transitional to *Epigondolella nodosa* (Hayashi), oblique lateral–upper view, ×50, *P. carpathica* Zone, Middle Tuvalian, 14.8 m, rep.-No. 31-3-98/I-12.
10. *Paragondolella carpathica* (Mock), oblique lateral–upper view, ×50, *P. carpathica* Zone, Middle Tuvalian, 28.8 m, rep.-No. 31-3-98/I-15.
11. *P. polygnathiformis noah* (Hayashi), lateral view, × 55, *P. carpathica* Zone, Middle Tuvalian, 12 m, rep.-No. 21-10-98/I-134.
12. *P. polygnathiformis noah* (Hayashi), oblique lateral–upper view, ×50, *P. carpathica* Zone, Middle Tuvalian, 33.5 m, rep.-No. 31-3-98/I-20.
13. *Paragondolella oertlii* (Kozur), upper view, ×50, *P. carpathica* Zone, Middle Tuvalian, 33.5 m, rep.-No. 31-3-98/I-21.
14. *Epigondolella nodosa* (Hayashi), primitive form, short morphotype, upper view, ×50, *E. nodosa* Zone, Upper Tuvalian, 39.5 m, rep.-No. 23-2-97/I-35.
15. *Epigondolella nodosa* (Hayashi), primitive form, upper view, ×60, *E. nodosa* Zone, Upper Tuvalian, 39.5 m, rep.-No. 21-10-98/I-139.
16. *Epigondolella nodosa zoae* (Orchard), oblique lateral–upper view, ×50, *E. nodosa* Zone, Upper Tuvalian, 39.5 m, rep.-No. 9-2-99/I-14.
17. *Epigondolella nodosa* (Hayashi), juvenile form, upper view, ×50, *E. nodosa* Zone, Upper Tuvalian, 39.5 m, rep.-No. 9-2-99/I-17.
18. *Paragondolella polygnathiformis noah (*Hayashi), juvenile form, oblique lateral view, ×50, *E. nodosa* Zone, Upper Tuvalian, 39.5 m, rep.-No. 31-3-98/I-26.
19. *Epigondolella nodosa* (Hayashi), long morphotype, morphologic transition field between *E. nodosa nodosa* (Hayashi) and *E. nodosa zoae* (Orchard), upper view, ×50, *E. nodosa* Zone, Upper Tuvalian, 39.5 m, rep.-No. 9-2-99/I-18.
20. *Epigondolella nodosa* (Hayashi), late juvenile stage, oblique lateral–upper view, ×50, *E. nodosa* Zone, Upper Tuvalian, 39.5 m, rep.-No. 31-3-98/I-24.
21. *Epigondolella nodosa* (Orchard), superadult *pseudodiebeli* stage but posterior part of platform without nodes, long morphotype, morphologic transition field between *E. nodosa nodosa* (Hayashi) and *E. nodosa zoae* (Orchard), upper view, ×50, *E. nodosa* Zone, Upper Tuvalian, 39.5 m, rep.-No. 9-2-99/I-15.
22. *Paragondolella polygnathiformis noah (*Hayashi), lateral view, ×50, *E. nodosa* Zone, Upper Tuvalian, 39.5 m, rep.-No. 31-3-98//I-25.
23. *Epigondolella nodosa* (Hayashi), late juvenile stage, oblique upper view, ×60, *E. nodosa* Zone, Upper Tuvalian, 40.0 m, rep.-No. 21-10-98/I-179.
24. *Epigondolella nodosa nodosa* (Hayashi), transitional form between short and long morphotypes, oblique lateral–upper view, ×50, *E. nodosa* Zone, Upper Tuvalian, 40.0 m, rep.-No. 21-10-98/I-194.
25. *Epigondolella nodosa nodosa* (Hayashi), short morphotype, upper view, ×50, *E. nodosa* Zone, Upper Tuvalian, 40.0 m, rep.-No. 9-2-99/I-32.
26. *Neocavitella cavitata* Budurov, oblique lateral–lower view, ×50, *E. nodosa* Zone, Upper Tuvalian, 40.0 m, rep.-No. 9-2-99/I-28.
27. *Paragondolella oertlii* (Kozur), upper view, ×50, *E. nodosa* Zone, Upper Tuvalian, 40.0 m, rep.-No. 9-2-99/I-30.
28. *Epigondolella nodosa* (Hayashi), juvenile form, oblique upper view, ×50, *E. nodosa* Zone, Upper Tuvalian, 40 m, rep.-No. 31-3-98/I-31.

Fig. A1 (*Continued*).

29. *Paragondolella polygnathiformis noah* (Hayashi), lateral view, ×50, *E. nodosa* Zone, Upper Tuvalian, 40.0 m, rep.-No. 21-10-98/I-193.
30. *Epigondolella nodosa* (Hayashi), juvenile form, oblique lateral view, ×65, *E. nodosa* Zone, Upper Tuvalian, 40 m, rep.-No. 21-10-98/I-180.
31. *Epigondolella nodosa nodosa* (Hayashi), long morphotype, upper view, ×55, *E. nodosa* Zone, Upper Tuvalian, 40.0 m, rep.-No. 21-10-98/I-182.
32. *Epigondolella nodosa nodosa* (Hayashi), long morphotype, upper view, ×55, *E. nodosa* Zone, Upper Tuvalian, 40.0 m, rep.-No. 21-10-98/I-181.
33. *Epigondolella nodosa* (Hayashi), late juvenile stage, upper view, ×50, *E. nodosa* Zone, Upper Tuvalian, 40.5 m, rep.-No. 1-4-98/I-1.
34. *Epigondolella nodosa zoae* (Orchard), upper view, ×50, *E. nodosa* Zone, Upper Tuvalian, 40.0 m, rep.-No. 31-3-98/I-39.
35. *Paragondolella*? *reversa* (Mosher), lower view, ×50, *E. nodosa* Zone, Upper Tuvalian, 40.5 m, rep.-No. 31-3-98/I-53.
36. *Paragondolella polygnathiformis noah (*Hayashi), lateral view, ×50, *E. nodosa* Zone, Upper Tuvalian, 40.5 m, rep.-No. 1-4-98/I-5.
37. *Epigondolella nodosa nodosa* (Hayashi), short morphotype, upper view, ×50, *E. nodosa* Zone, Upper Tuvalian, 40.5 m, rep.-No. 1-4-98/I-4.
38. *Epigondolella nodosa nodosa* (Hayashi), long morphotype, upper view, ×50, *E. nodosa* Zone, Upper Tuvalian, 41.8 m, rep.-No. 1-4-98/I-29.
39. *Epigondolella nodosa zoae* (Orchard), upper view, ×50, *E. nodosa* Zone, Upper Tuvalian, 41.8 m, rep.-No. 1-4-98/I-45.
40. *Epigondolella permica* (Hayashi), juvenile stage, upper view, ×50, *E. pseudodiebeli* Zone, Upper Tuvalian, 43.5 m, rep.-No. 1-4-98/I-50.
41. *Paragondolella oertlii* (Kozur), upper view, ×50, *E. nodosa* Zone, Upper Tuvalian, 41.8 m, rep.-No. 1-4-98/I-21.
42. *Epigondolella permica* (Hayashi), upper view, ×50, lowermost *E. primitia* Zone, uppermost Tuvalian, 44.6 m, rep.-No. 1-4-98/I-55.
43. *Epigondolella pseudodiebeli* (Kozur), juvenile form, upper view, ×50, *E. pseudodiebeli* Zone, Upper Tuvalian, 44.0 m, rep.-No. 1-4-98/I-61.
44. *Epigondolella primitia* Mosher, oblique lateral view, ×50, lowermost *E. primitia* Zone, uppermost Tuvalian, 44.6 m, rep.-No. 31-3-98/I-61.
45. *Epigondolella pseudodiebeli* (Kozur), short morphotype, upper view, ×50, *E. pseudodiebeli* Zone, Upper Tuvalian, 43.5 m, rep.-No. 1-4-98/I-47.
46. *Epigondolella permica* (Hayashi), juvenile form, upper view, ×50, *E. pseudodiebeli* Zone, Upper Tuvalian, 44.0 m, rep.-No. 1-4-98/I-69
47. *Epigondolella pseudodiebeli* (Kozur), upper view, ×50, lowermost *E. primitia* Zone, uppermost Tuvalian, 44.6 m, rep.-No. 1-4-98/I-78
48. *Epigondolella pseudoechinata* Kozur, upper view, ×50, lowermost *E. primitia* Zone, uppermost Tuvalian, 44.6 m, rep.-No. 31-3-98/I-57.
49. *Epigondolella pseudoechinata* Kozur, upper view, ×50, lowermost *E. primitia* Zone, uppermost Tuvalian, 44.6 m, rep.-No. 21-10-98/I-202.
50. *Epigondolella pseudodiebeli* (Kozur), short morphotype, upper view, ×50, lowermost *E. primitia* Zone, uppermost Tuvalian, 44.6 m, rep.-No. 21-10-98/I-201.
51. *Epigondolella pseudodiebeli* (Kozur), late juvenile stage, upper view, ×50, lowermost *E. primitia* Zone, uppermost Tuvalian, 44.6 m, rep.-No. 1-4-98/I-70.
52. *Epigondolella primitia* Mosher, primitive form, upper view, ×50, lowermost *E. primitia* Zone, uppermost Tuvalian, 44.6 m, rep.-No. 31-3-98/I-62.
53. *Epigondolella primitia* Mosher, primitive form, upper view, ×50, lowermost *E. primitia* Zone, uppermost Tuvalian, 44.6 m, rep.-No. 31-3-98/I-55.
54. *Epigondolella permica* (Hayashi), upper view, ×50, lowermost *E. primitia* Zone, uppermost Tuvalian, 44.6 m, rep.-No. 1-4-98/I-76.
55. *Epigondolella primitia* Mosher, juvenile form, upper view, ×50, lower *E. primitia* Zone, uppermost Tuvalian, 45.4 m, rep. No. 21-10-98/I-198.
56. *Epigondolella permica* (Hayashi), upper view, ×50, lowermost *E. primitia* Zone, uppermost Tuvalian, 44.6 m, rep.-No. 1-4-98/I-71.

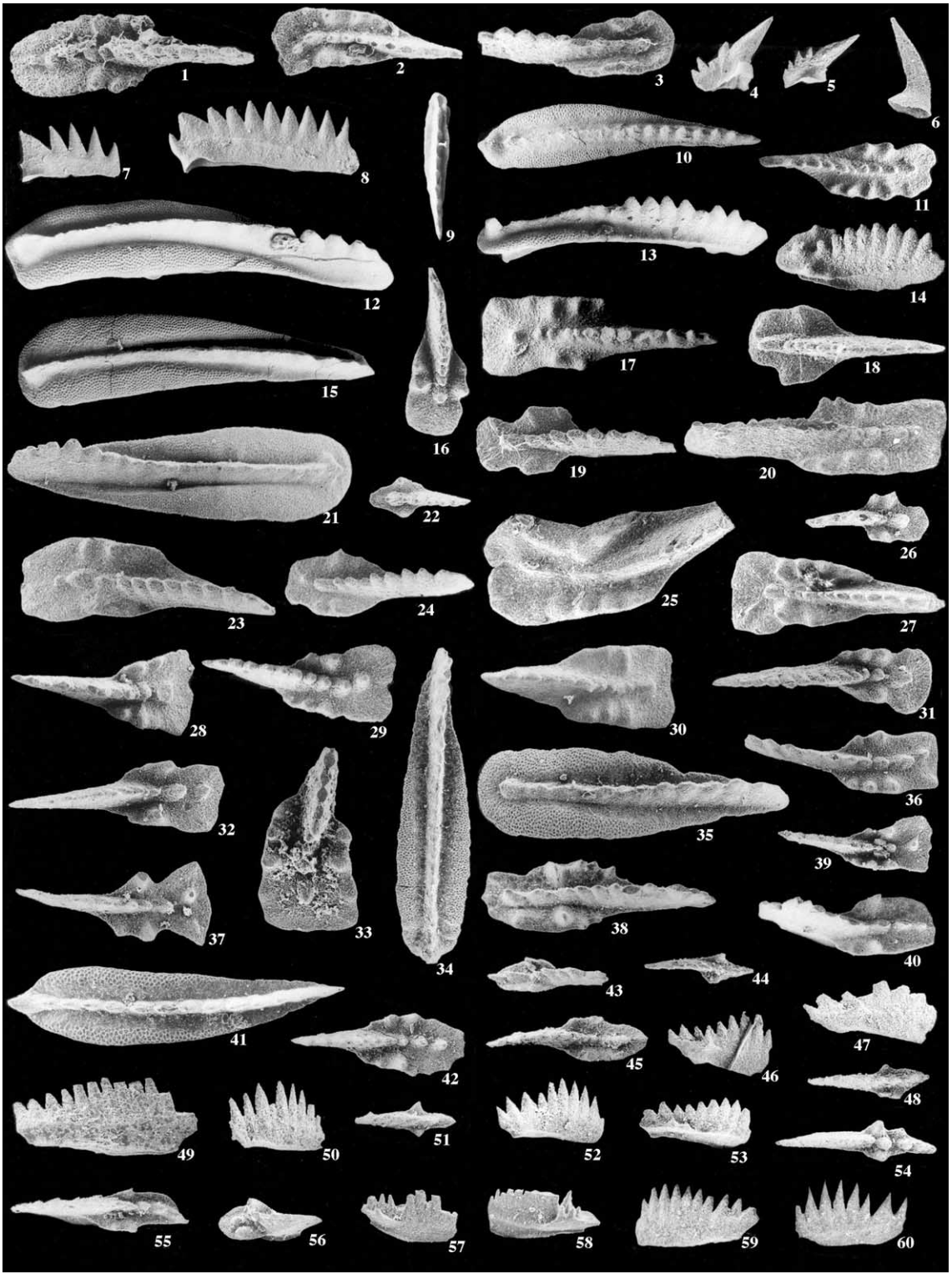
1
2
3
4
5
6
7
8
9
10
11
12
13
14
15
16
17
18
19
20
21
22
23
24
25
26
27
28
29
30
31
32
33
34
35
36
37
38
39
40
41
42
43
44
45
46
47
48
49
50
51
52
53
54
55
56
57
58
59
60

Fig. A2.

Fig. A2. All illustrated specimens are from the trench section near Silická Brezová. The meter levels indicate m above the base of the trench section.

1. *Epigondolella* cf. *primitia* Mosher, upper view, ×55, lower *E. primitia* Zone, uppermost Tuvalian, 45.4 m, rep.-No. 21-10-98/I-115.
2. *Epigondolella primitia* Mosher, upper view, ×65, lower *E. primitia* Zone, uppermost Tuvalian, 46.0 m, rep.-No. 21-10-98/I-20A.
3. *Epigondolella primitia* Mosher, upper view, ×65, lower *E. primitia* Zone, uppermost Tuvalian, 45.4 m, rep.-No. 21-10-98/I-196.
4. *Misikella longidentata* Kozur and Mock, ×50, lower *E. primitia* Zone, uppermost Tuvalian, 44,6 m, rep.-No. 9-2-99/I-54.
5. *Misikella longidentata* Kozur and Mock, ×50, upper *E. primitia* Zone, lowermost Norian, 46.5 m, rep.-No. 22-10-98/II-25.
6. *Zieglericonus* n. sp., ×50, *E. abneptis* Zone, Middle Lacian (Lower Norian), 53.4 m, rep.-No. 3-4-98/III-5.

7–10, 12, 13. *Norigondolella navicula* (Huckriede), different ontogenetic stages, all from the upper *E. primitia* Zone, lowermost Norian, 46.5 m

7. Earliest juvenile stage, without platform, lateral view, ×60, rep.-No. 22-10-98/II-27
8. Early juvenile stage, with beginning platform development (very narrow ridge in the middle part of the unit), lateral view, ×60, rep.-No. 22-10-98/II-13
9. Early juvenile stage, with fully developed but still very narrow platform, posterior brim not yet present, upper view, ×50, rep.-No. 22-10-98/II-21
10. Late juvenile stage, large specimen with narrow platform, without posterior brim, beginning fusion of the posterior part of the carina, upper view, ×50, rep.-No. 22-10-98/II-3
12. Adult, very large specimen, platform well developed, with distinct brim, two-thirds of the carina is fused to a smooth ridge, oblique upper view, ×40, rep.-No. 22-10-98/II-19.
13. Subadult stage, large specimen with moderately wide platform which has a distinct posterior brim, posterior third of the carina fused to a smooth ridge, oblique lateral view, ×50, rep.-No. 22-10-98/II-5.
11. *Epigondolella permica* (Hayashi), upper view, ×60, upper *E. primitia* Zone, lowermost Norian, 49.2 m, rep.-No. 22-10-98/II-59.
14. *Epigondolella pseudoechinata* Kozur, oblique lateral–upper view, ×60, upper *E. primitia* Zone, lowermost Norian, 49.2 m, rep.-No. 22-10-98/II-44.
15. *Norigondolella navicula* (Huckriede), upper view, ×40, upper *E. primitia* Zone, lowermost Norian, 47 m, rep.-No. 22-10-98/II-36.
16. *Epigondolella abneptis* (Huckriede), subadult specimen, upper view, ×50, *E. abneptis* Zone, Middle Lacian (Lower Norian), 49.5 m, rep.-No. 9-2-99/I-69.
17. *Epigondolella abneptis* (Huckriede), upper view, ×55, *E. abneptis* Zone, Middle Lacian (Lower Norian), 49.5 m, rep.-No. 22-10-98/II-63.
18. *Epigondolella pseudoechinata* Kozur, upper view, ×65, *E. abneptis* Zone, Middle Lacian (Lower Norian), 49.5 m, rep.-No. 22-10-98/II-73.
19. *Epigondolella permica* (Hayashi), upper view, ×50, *E. abneptis* Zone, Middle Lacian (Lower Norian), 50.0 m, rep.-No. 22-10-98/II-90.
20. *Epigondolella primitia* Mosher, upper view, ×50, *E. abneptis* Zone, Middle Lacian (Lower Norian), 51.0 m, rep.-No. 22-10-98/II-112.
21. *Norigondolella navicula* (Huckriede), upper view, ×50, *E. abneptis* Zone, Middle Lacian (Lower Norian), 50.0 m, rep.-No. 22-10-98/II-87.
22. *Epigondolella abneptis* (Huckriede), early juvenile stage, upper view, ×50, *E. abneptis* Zone, Middle Lacian (Lower Norian), 53,4 m, rep.-No. 3-4-98/III-9.
23. *Epigondolella abneptis* (Huckriede), upper view, ×50, *E. abneptis* Zone, Middle Lacian (Lower Norian), 51 m, rep.-No. 22-10-98/II-107.
24. *Epigondolella pseudoechinata* Kozur, upper view, ×50, *E. abneptis* Zone, Middle Lacian (Lower Norian), 51 m, rep.-No. 22-10-98/II-113.
25. *Epigondolella abneptis* (Huckriede), upper view, ×50, *E. abneptis* Zone, Middle Lacian (Lower Norian), 51.0 m, rep.-No. 22-10-98/II-106.
26. *Epigondolella abneptis* (Huckriede), juvenile stage, upper view, ×50, *E. abneptis* Zone, Middle Lacian (Lower Norian), 53.7 m, rep.-No. 3-4-98/III-11.
27. *Epigondolella abneptis* (Huckriede), upper view, ×60, *E. abneptis* Zone, Middle Lacian (Lower Norian), 51.0 m, rep.-No. 22-10-98/II-110.

Fig. A2 (*Continued*).

28. *Epigondolella abneptis* (Huckriede), upper view, ×50, *E. abneptis* Zone, Middle Lacian (Lower Norian), 52.0 m, rep.-No. 22-10-98/II-135.
29. *Epigondolella abneptis* (Huckriede), upper view, ×50, *E. abneptis* Zone, Middle Lacian (Lower Norian), 52.0 m, rep.-No. 22-10-98/II-132.
30. *Epigondolella abneptis* (Huckriede), upper view, ×50, *E. abneptis* Zone, Middle Lacian (Lower Norian), 52.0 m, rep.-No. 22-10-98/II-129.
31. *Epigondolella abneptis* (Huckriede), upper view, ×50, *E. abneptis* Zone, Middle Lacian (Lower Norian), 53.4 m, rep.-No. 3-4-98/III-3.
32. *Epigondolella abneptis* (Huckriede), upper view, ×50, lowermost *E. triangularis* Zone, Upper Lacian (Lower Norian), 54 m, rep.-No. 2-4-98/II-49.
33. *Epigondolella abneptis* (Huckriede), upper view, ×50, lowermost *E. triangularis* Zone, Upper Lacian (Lower Norian), 54 m, rep.-No. 2-4-98/II-30.
34. *Norigondolella navicula* (Huckriede), advanced form, upper view, ×50, lowermost *E. triangularis* Zone, Upper Lacian (Lower Norian), 54 m, rep.-No. 2-4-98/II-8.
35. *Norigondolella navicula* (Huckriede), upper view, ×50, lowermost *E. triangularis* Zone, Upper Lacian (Lower Norian), 54 m, rep.-No. 2-4-98/II-20,
36. *Epigondolella abneptis* (Huckriede), upper view, ×50, lowermost *E. triangularis* Zone, Upper Lacian (Lower Norian), 54 m, rep.-No. 2-4-98/II-31.
37. *Epigondolella abneptis* (Huckriede), upper view, ×50, lowermost *E. triangularis* Zone, Upper Lacian (Lower Norian), 54 m, rep.-No. 2-4-98/II-31B.
38. *Epigondolella spiculata* Orchard, upper view, ×50, *E. spiculata* Zone, Upper Alaunian (upper part of Middle Norian), fissure filling, 54.3 m, rep.-No. 22-10-98/II-153.
39. *Epigondolella triangularis* (Budurov), very primitive form, upper view, ×50, lowermost *E. triangularis* Zone, Upper Lacian (Lower Norian), 54 m, rep.-No. 2-4-98/II-37.
40. *Mockina* cf. *medionorica* Kozur, n. sp., upper view, ×50, *E. spiculata* Zone, Upper Alaunian (upper part of Middle Norian), fissure filling, 54.5 m, rep.-No. 9-2-99/I-77.
41. *Norigondolella steinbergensis* (Mosher), upper view, ×50, *E. spiculata* Zone, Upper Alaunian (upper part of Middle Norian), fissure filling, 54.3 m, rep.-No. 22-10-98/II-146.
42. *Epigondolella spiculata* Orchard, upper view, ×50, *E. spiculata* Zone, Upper Alaunian (upper part of Middle Norian), fissure filling, 54.5 m, rep.-No. 9-2-99/I-78.
43. *Mockina zapfei* (Kozur), somewhat oblique upper view, ×50, *M. bidentata* Zone, Sevatian, 57.0 m, rep.-No. 9-2-99/I-90.
44. *Mockina bidentata* (Mosher), upper view, ×50, *M. bidentata* Zone, Sevatian, 57.0 m, rep.-No. 9-2-99/I-89.
45. *Mockina zapfei* (Kozur), upper view, ×50, *M. bidentata* Zone, Sevatian, 57.0 m, rep.-No. 9-2-99/I-87.
46. *Mockina bidentata* (Mosher), lateral view, ×50, *M. bidentata* Zone, Sevatian, 57.0 m, rep.-No. 9-2-99/I-86.
47. *Mockina bidentata* (Mosher), lateral view, ×75, *M. bidentata* Zone, Sevatian, 57.0 m, rep.-No. 9-2-99/I-98.
48. *Mockina bidentata* (Mosher), upper view, ×50, *M. bidentata* Zone, Sevatian, 57.0 m, rep.-No. 9-2-99/I-88.
49. *Parvigondolella vrielyncki* Kozur and Mock, lateral view, ×60, upper *M. bidentata* Zone, Sevatian, 59.0 m, rep.-No. 22-10-98/III-1.
50. *Parvigondolella andrusovi* Kozur and Mock, lateral view, ×50, upper *M. bidentata* Zone, Sevatian, 62.0 m, rep.-No. 22-10-98/III-15.
51. *Mockina bidentata* (Mosher), upper view, ×50, upper *M. bidentata* Zone, Sevatian, 62.5 m, rep.-No. 9-2-99/I-195.
52. *Parvigondolella andrusovi* Kozur and Mock, lateral view, ×50, upper *M. bidentata* Zone, Sevatian, 62.7 m, rep.-No. 9-2-99/I-234.
53. *Mockina zapfei* (Kozur), lateral view, ×50, upper *M. bidentata* Zone, Sevatian, 63.5 m, rep.-No. 22-10-98/III-67.
54. *Mockina bidentata* (Mosher), upper view, ×50, upper *M. bidentata* Zone, Sevatian, 63.5 m, rep.-No. 22-10-98/III-68.
55. *Mockina zapfei* Kozur, advanced specimen, upper view, ×50, *P. andrusovi* Zone, Sevatian, 63.7 m, rep.-No. 9-2-99/II-5.
56. *Mockina slovakensis* (Kozur), advanced specimen, somewhat oblique upper view, ×50, *P. andrusovi* Zone, Sevatian, 63.7 m, rep.-No. 9-2-99/II-8.
57. *Mockina slovakensis* (Kozur), advanced specimen, somewhat oblique lateral view, ×50, *P. andrusovi* Zone, Sevatian, 63.7 m, rep.-No. 3-4-98/III-72.
58. *Mockina slovakensis* (Kozur), advanced specimen, lateral view, ×50, *P. andrusovi* Zone, Sevatian, 63.7 m, rep.-No. 9-2-99/II-20.
59. *Parvigondolella andrusovi* Kozur and Mock, lateral view, ×50, *P. andrusovi* Zone, Sevatian, 63.7 m, rep.-No. 9-2-99/II-61.
60. *Parvigondolella andrusovi* Kozur and Mock, lateral view, ×50, *P. andrusovi* Zone, Sevatian, 63.7 m, rep.-No. 9-2-99/II-51.

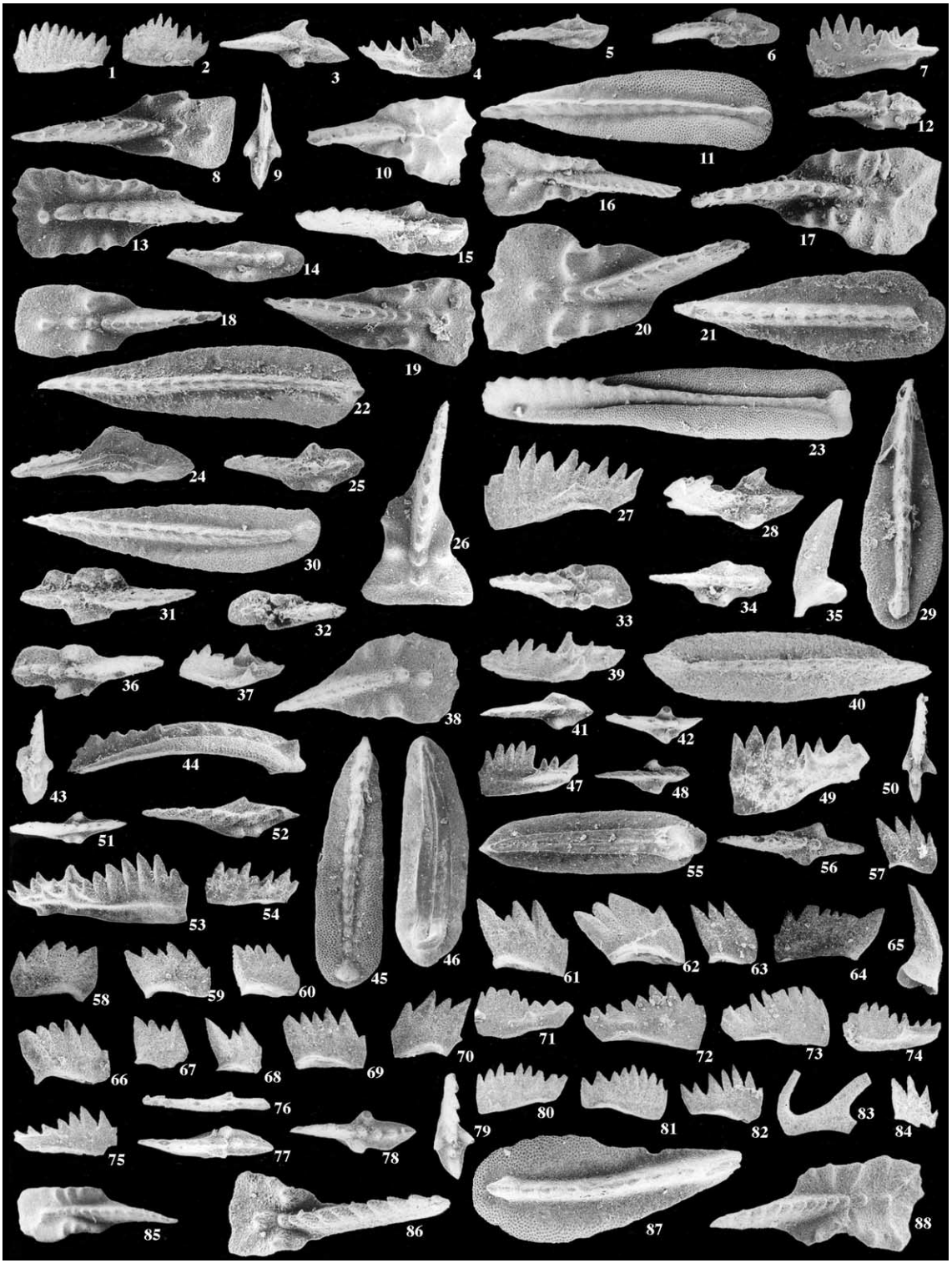
1
2
3
4
5
6
7
8
9
10
11
12
13
14
15
16
17
18
19
20
21
22
23
24
25
26
27
28
29
30
31
32
33
34
35
36
37
38
39
40
41
42
43
44
45
46
47
48
49
50
51
52
53
54
55
56
57
58
59
60
61
62
63
64
65
66
67
68
69
70
71
72
73
74
75
76
77
78
79
80
81
82
83
84
85
86
87
88

Fig. A3.

Fig. A3. The illustrated specimens, except numbers 85-88, are from the trench section near Silická Brezová. The meter levels indicate m above the base of the trench section. Specimens 85-88 are from the quarries.

1. *Parvigondolella andrusovi* Kozur and Mock, lateral view, ×50, *P. andrusovi* Zone, Sevatian, 63.7 m, rep.-No. 9-2-99/II-56.
2. *Parvigondolella andrusovi* Kozur and Mock, lateral view, ×50, *P. andrusovi* Zone, Sevatian, 63.7 m, rep.-No. 9-2-99/II-55.
3. *Mockina bidentata* (Mosher), upper view, ×50, *M. bidentata* Zone, Sevatian *Halorella*-bearing fissure filling within Lower–Middle Norian brecciated limestone, 65.0 m, rep.-No. 22-10-98/III-114.
4. *Mockina bidentata* (Mosher), lateral view, ×50, *M. bidentata* Zone, Sevatian *Halorella*-bearing fissure filling within Lower–Middle Norian brecciated limestone, 65.0 m, rep.-No. 22-10-98/III-116.
5. *Mockina zapfei* (Kozur), upper view, ×50, *M. bidentata* Zone, Sevatian fissure filling in Lower–Middle Norian brecciated limestone, 66.0 m, rep.-No. 22-10-98/III-163.
6. *Mockina bidentata* (Mosher), primitive form, upper view, ×50, *M. bidentata* Zone, Sevatian fissure filling in Lower–Middle Norian brecciated limestone, 66.0 m, rep.-No. 22-10-98/III-162.
7. *Mockina bidentata* (Mosher), lateral view, ×50, *M. bidentata* Zone, Sevatian fissure filling in Lower–Middle Norian brecciated limestone, 66.0 m, rep.-No. 22-10-98/III-164.
8. *Epigondolella abneptis* (Huckriede), upper view, ×55, *E. abneptis* Zone, Middle Lacian, 70 m, rep.-No. 22-10-98/III-185.
9. *Mockina bidentata* (Mosher), upper view, ×50, Sevatian fissure filling within Lower–Middle Norian brecciated limestone, 72 m, rep.-No. 22-10-98/III-210.
10. *Epigondolella triangularis* (Budurov), upper view, ×50, Lower–Middle Norian brecciated limestone, 73 m, rep.-No. 9-2-99/II-81.
11. *Norigondolella navicula* (Huckriede), upper view, ×50, Lower–Middle Norian brecciated limestone, 73 m, rep.-No. 9-2-99/II-93.
12. *Mockina* cf. *carinata* (Orchard), upper view, ×50, Lower–Middle Norian brecciated limestone, 74 m, rep.-No. 9-2-99/II-109.
13. *Epigondolella triangularis uniformis* Orchard, upper view, ×50, Lower–Middle Norian brecciated limestone, 76.9 m, rep.-No. 3-4-98/III-78.
14. *Mockina medionorica* Kozur, n. sp., holotype, upper view, ×50, Middle Norian brecciated limestone, 78 m, rep.-No. 9-2-99/II-126.
15. *Mockina medionorica* Kozur, n. sp., upper view, ×50, Middle Norian brecciated limestone, 80 m, rep.-No. 9-2-99/II-148.
16. *Epigondolella triangularis* (Budurov), upper view, ×50, Lower–Middle Norian brecciated limestone, 74 m, rep.-No. 9-2-99/II-97.
17. *Epigondolella triangularis* (Budurov), upper view, ×50, Lower–Middle Norian brecciated limestone, 76 m, rep.-No. 9-2-99/II-117.
18. *Epigondolella abneptis* (Huckriede), upper view, ×50, Middle Norian brecciated limestone, 79 m, rep.-No. 9-2-99/II-142.
19. *Epigondolella triangularis uniformis* Orchard, upper view, ×50, Middle Norian brecciated limestone, 80 m, rep.-No. 9-2-99/II-152.
20. *Epigondolella triangularis* (Budurov), upper view, ×50, Middle Norian brecciated limestone, 79 m, rep.-No. 9-2-99/II-133.
21. *Norigondolella hallstattensis* (Mosher), upper view, ×50, Middle Norian brecciated limestone, 79 m, rep.-No. 9-2-99/II-135.
22. *Norigondolella steinbergensis* (Mosher, upper view, ×50, Middle Norian brecciated limestone, 79 m, rep.-No. 9-2-99/II-134.
23. *Norigondolella steinbergensis* (Mosher), oblique upper view, ×40, *M. postera* Zone, Upper Alaunian, 84 m, rep.-No. 9-2-99/II-177.
24. *Mockina zapfei* (Kozur), somewhat oblique lower view, ×50, basal *M. bidentata* Zone, lowermost Sevatian, 85.2 m, rep.-No. 23-10-98/IV-117.
25. *Mockina bidentata* (Mosher), transitional form to *Mockina zapfei* (Kozur), upper view, ×50, basal *M. bidentata* Zone, lowermost Sevatian, 85.2 m, rep.-No. 23-10-98/IV-116.
26. *Epigondolella abneptis* (Huckriede), upper view, ×50, *M. postera* Zone, Upper Alaunian with reworked Lower Norian conodonts, 82.9 m, rep.-No. 9-2-99/II-169.
27. *Mockina bidentata* (Mosher), lateral view, ×50, basal *M. bidentata* Zone, lowermost Sevatian, 85.2 m, rep.-No. 23-10-98/IV-121.
28. *Mockina bidentata* (Mosher), somewhat oblique upper view, ×50, basal *M. bidentata* Zone, lowermost Sevatian, 85.2 m, rep.-No. 23-10-98/IV-120.

Fig. A3 (*Continued*).

29. *Norigondolella hallstattensis* (Mosher), upper view, ×50, *M. postera* Zone, Upper Alaunian, with few reworked Lower Norian conodonts, 84 m, rep.-No. 9-2-99/II-176.
30. *Norigondolella steinbergensis* (Mosher), upper view, ×50, basal *M. bidentata* Zone, lowermost Sevatian, 85.2 m, rep.-No. 23-10-98/IV-108.
31. *Mockina* cf. *zapfei* (Kozur), upper view, ×50, lower *M. bidentata* Zone, lowermost Sevatian, 85.7 m, rep.-No. 28-4-98/IV-117.
32. *Mockina zapfei* (Kozur), upper view, ×50, lower *M. bidentata* Zone, lowermost Sevatian, 85.7 m, rep.-No. 28-4-98/IV-13.
33. *Mockina zapfei* (Kozur), upper view, ×50, basal *M. bidentata* Zone, lowermost Sevatian, 85.2 m, rep.-No. 23-10-98/IV-118.
34. *Mockina zapfei* (Kozur), upper view, ×50, basal *M. bidentata* Zone, lowermost Sevatian, 85.2 m, rep.-No. 23-10-98/IV-114.
35. *Zieglericonus* n. sp., ×50, basal *M. bidentata* Zone, lowermost Sevatian, 85.2 m, rep.-No. 23-10-98/IV-99.
36. *Mockina zapfei* (Kozur), upper view, ×50, lower *M. bidentata* Zone, Lower Sevatian, 85.7 m, rep.-No. 28-4-99/I-116.
37. *Mockina bidentata* (Mosher), oblique upper view, ×50, lower *M. bidentata* Zone, Lower Sevatian, 85.8 m, rep.-No. 28-4-99/I-90.
38. *Epigondolella triangularis* (Budurov), upper view, ×50, reworked in lower *M. bidentata* Zone, Lower Sevatian, 85.8 m, rep.-No. 28-4-99/I-93.
39. *Mockina bidentata* (Mostler), oblique upper view, ×50, lower *M. bidentata* Zone, Lower Sevatian, 85.8 m, rep.-No. 28-4-99/I-97.
40. *Norigondolella steinbergensis* (Mosher), upper view, ×50, lower *M. bidentata* Zone, Lower Sevatian, 85.8 m, rep.-No. 28-4-99/I-98.
41. *Mockina bidentata* (Mostler), upper view, ×50, *M. bidentata* Zone, Sevatian, 90 m, rep.-No. 28-4-99/I-27.
42. *Mockina bidentata* (Mostler), upper view, ×50, *M. bidentata* Zone, Sevatian, 90 m, rep.-No. 28-4-99/I-23.
43. *Mockina zapfei* (Kozur), juvenile specimen, upper view, ×50, lower *M. bidentata* Zone, Lower Sevatian, 85.8 m, rep.-No. 28-4-99/I-99.
44. *Norigondolella kozuri* (Gedik), lateral view, ×50, lower *M. bidentata* Zone, Lower Sevatian, 89 m, rep.-No. 9-2-99/II-271A.
45. *Norigondolella kozuri* (Gedik), upper view, ×50, lower *M. bidentata* Zone, Lower Sevatian, 89 m, rep.-No. 9-2-99/II-269.
46. *Norigondolella kozuri* (Gedik), lower view, ×50, lower *M. bidentata* Zone, Lower Sevatian, 89 m, rep.-No. 9-2-99/II-268.
47. *Mockina bidentata* (Mostler), lateral view, ×50, *M. bidentata* Zone, Sevatian, 91 m, rep.-No. 28-4-99/I-13.
48. *Mockina bidentata* (Mostler), upper view, ×50, *M. bidentata* Zone, Sevatian, 91 m, rep.-No. 28-4-99/I-11.
49. *Mockina* cf. *slovakensis* (Kozur), lateral view, ×50, *M. bidentata* Zone, Sevatian, 91 m, rep.-No. 28-4-99/I-9.
50. *Mockina bidentata* (Mostler), upper view, ×50, *M. bidentata* Zone, Sevatian, 91 m, rep.-No. 28-4-99/I-1.
51. *Mockina zapfei* (Kozur), transitional form to *M. bidentata* (Mosher), late juvenile stage, upper view, ×50, *M. bidentata* Zone, Sevatian, 91 m, rep.-No. 28-4-99/I-10A.
52. *Mockina zapfei* (Kozur), advanced form, transitional form to *M. bidentata* (Mosher), upper view, ×50, *M. bidentata* Zone, Sevatian, 91 m, rep.-No. 9-2-99/II-275.
53. *Mockina zapfei* (Kozur), lateral view, ×50, *M. bidentata* Zone, Sevatian, 91 m, rep.-No. 28-4-99/I-4A.
54. *Mockina bidentata* (Mosher), lateral view, ×50, *M. bidentata* Zone, Sevatian, 94.9 m, rep.-No. 9-2-99/II-289.
55. *Norigondolella kozuri* (Gedik), lower view, ×50, *M. bidentata* Zone, Sevatian, 94.1 m, rep.-No. 9-2-99/II-282.
56. *Mockina bidentata* (Mostler), upper view, ×50, *M. hernsteini* Zone, Upper Sevatian, 106.8 m, rep.-No. 9-2-99/II-356.
57. *Misikella hernsteini* (Mostler), lateral view, ×50, *M. hernsteini* Zone, Upper Sevatian, 106.8 m, rep.-No. 9-2-99/II-317.
58. *Misikella hernsteini* (Mostler), lateral view, ×50, *M. hernsteini* Zone, Upper Sevatian, 106.8 m, rep.-No. 9-2-99/II-355.
59. *Misikella hernsteini* (Mostler), lateral view, ×50, *M. hernsteini* Zone, Upper Sevatian, 106.8 m, rep.-No. 9-2-99/II-316.
60. *Misikella hernsteini* (Mostler), lateral view, ×50, *M. hernsteini* Zone, Upper Sevatian, 106.8 m, rep.-No. 9-2-99/IV-14.
61. *Misikella hernsteini* (Mostler), lateral view, ×50, *M. hernsteini* Zone, Upper Sevatian, 106.8 m, rep.-No. 9-2-99/II-342.
62. *Misikella hernsteini* (Mostler), lateral view, ×50, *M. hernsteini* Zone, Upper Sevatian, 106.8 m, rep.-No. 23-10-98/IV-11.
63. *Misikella hernsteini* (Mostler), lateral view, ×50, *M. hernsteini* Zone, Upper Sevatian, 106.8 m, rep.-No. 9-2-99/II-334.
64. *Parvigondolella lata* Kozur and Mock, lateral view, ×50, *M. hernsteini* Zone, Upper Sevatian, 106.8 m, rep.-No. 9-2-99/II-357.
65. *Zieglericonus* sp., ×50, *M. hernsteini* Zone, Upper Sevatian, 106.8 m, rep.-No. 9-2-99/II-345.
66. *Misikella hernsteini* (Mostler), lateral view, ×50, *M. hernsteini* Zone, Upper Sevatian, 106.8 m, rep.-No. 9-2-99/II-349.

Fig. A3 (*Continued*).

67. *Misikella hernsteini* (Mostler), lateral view, ×50, *M. hernsteini* Zone, Upper Sevatian, 106.8 m, rep.-No. 9-2-99/II-350.
68. *Misikella hernsteini* (Mostler), lateral view, ×50, *M. hernsteini* Zone, Upper Sevatian, 106.8 m, rep.-No. 9-2-99/II-347.
69. *Misikella hernsteini* (Mostler), lateral view, ×50, *M. hernsteini* Zone, Upper Sevatian, 106.8 m, rep.-No. 9-2-99/IV-12.
70. *Misikella hernsteini* (Mostler), lateral view, ×50, *M. hernsteini* Zone, Upper Sevatian, 106.8 m, rep.-No. 9-2-99/II-315.
71. *Mockina bidentata* (Mostler), lateral view, ×50, *M. hernsteini* Zone, Upper Sevatian, 108.1 m, rep.-No. 23-10-98/IV-33.
72. *Mockina bidentata* (Mostler), advanced form with strongly reduced lateral denticle on one side, lateral view, ×50, *M. hernsteini* Zone, Upper Sevatian, 108.1 m, rep.-No. 23-10-98/IV-29.
73. *Parvigondolella andrusovi* Kozur and Mock, lateral view, ×50, *M. hernsteini* Zone, Upper Sevatian, 109.6 m, rep.-No. 23-10-98/IV-46.
74. *Mockina bidentata* (Mostler), lateral view, ×50, *M. hernsteini* Zone, Upper Sevatian, 110.1 m, rep.-No. 23-10-98/IV-52.
75. *Mockina bidentata* (Mostler), lateral view, ×50, *M. hernsteini* Zone, Upper Sevatian, 112.2 m, rep.-No. 9-2-99/II-355.
76. *Mockina bidentata* (Mostler), advanced form, lateral denticle only on one side, upper view, ×50, *M. hernsteini* Zone, Upper Sevatian, 112.2 m, rep.-No. 23-10-97/IV-70.
77. *Mockina bidentata* (Mostler), upper view, ×50, *M. hernsteini* Zone, Upper Sevatian, 112.4 m, rep.-No. 23-10-97/IV-60.
78. *Mockina bidentata* (Mostler), upper view, ×50, *M. hernsteini* Zone, Upper Sevatian, 112.4 m, rep.-No. 23-10-97/IV-51.
79. *Mockina bidentata* (Mostler), upper view, ×50, *M. hernsteini* Zone, Upper Sevatian, 112.4 m, rep.-No. 23-10-98/IV-65.
80. *Parvigondolella andrusovi* Kozur and Mock, lateral view, ×50, *M. hernsteini* Zone, Upper Sevatian, 112.4 m, rep.-No. 23-10-98/IV-81.
81. *Parvigondolella andrusovi* Kozur and Mock, lateral view, ×50, *M. hernsteini* Zone, Upper Sevatian, 112.4 m, rep.-No. 23-10-98/IV-82.
82. *Parvigondolella andrusovi* Kozur and Mock, lateral view, ×50, *M. hernsteini* Zone, Upper Sevatian, 112.4 m, rep.-No. 23-10-98/IV-59.
83. *Oncodella paucidentata* (Mostler), ×50, *M. hernsteini* Zone, Upper Sevatian, 120.4 m, rep.-No. 23-10-98/IV-96.
84. *Misikella hernsteini* (Mostler), lateral view, ×50, *M. hernsteini* Zone, Upper Sevatian, 106.8 m, 120.4 m, rep.-No. 23-10-98/IV-95.
85. *Epigondolella abneptis* (Huckriede), upper view, ×40, Massiger Hellkalk quarry at 9 m, *E. abneptis* Zone, Middle Lacian, 25-4-00/I-1
86. *Epigondolella abneptis* (Huckriede), upper view, ×40, lower quarry at 1.4 m, *E. abneptis* Zone, Middle Lacian, 21-10-98/I-18.
87. *Norigondolella hallstattensis* (Mosher), upper view, ×50, *E. triangularis* Zone, Upper Lacian, frontal quarry at 25.8 m, rep.-No. 21-10-98/I-89.
88. *Epigondolella triangularis* (Budurov), upper view, ×50, *E. triangularis* Zone, Upper Lacian, frontal quarry at 17.6 m, rep.-No. 9-2-99/51.

Appendix

See Figs. A1–3.

References

Bock, W., 1953a. American Triassic estherids. J. Paleontol. 27, 62–76.

Bock, W., 1953b. *Howellisaura*, new name for *Howellites* BOCK. J. Paleontol. 27, 759.

Briden, J.C., Daniels, B.A., 1999. Palaeomagnetic correlation of the Upper Triassic of Somerset, England, with continental Europe and eastern North America. J. Geol. Soc. Lond. 156, 317–326.

Budurov, K.J., Sudar, M.N., 1990. Late Triassic conodont stratigraphy. Cour. Forsch.-Inst. Senckenberg 118, 203–239.

Bystrický, J., 1964. Slovenský kras. Dionyz Stúr Geological Institute, Bratislava, 304 pp.

Carter, E.S., Orchard, M.J., 2000. Intercalibrated conodont–radiolarian biostratigraphy and potential datums for the Carnian–Norian boundary within the Upper Triassic Peril Formation, Queen Charlotte Islands, British Columbia. In: Geological Survey of Canada, Current Research, 2000-A07, 11 pp.

Catalano, R., Di Stefano, P., Gullo, M., Kozur, H., 1990. Pseudofurnishius (Conodonta) in pelagic Late Ladinian–Early Carnian sediments of western Sicily and its stratigraphic and paleogeographic significance. Boll. Soc. Geol. Ital. 109, 91–101.

Channell, J.E.T., Kozur, H.W., 1997. How many oceans? Meliata, Vardar and Pindos oceans in Mesozoic Alpine paleogeography. Geology 25, 183–186.

Cornet, B., 1993. Applications and limitations of palynology in age, climatic and paleoenvironmental analyses of Triassic sequences in North America. In: Lucas, S.G., Morales, M.

(Eds.), The Non-Marine Triassic. New Mexico Museum of Natural History and Science, Bulletin 3, pp. 75–93.
Gallet, Y., Besse, J., Krystyn, L., Marcoux, J., Theveniaut, H., 1992. Magnetostratigraphy of the Late Triassic Bolücektası Tepe section (southwestern Turkey): implications for changes in magnetic reversal frequency. Phys. Earth Planet. Inter. 73, 85–108.
Gallet, Y., Besse, J., Krystyn, L., Theveniaut, H., Marcoux, J., 1993. Magnetostratigraphy of the Kavur Tepe section (southwestern Turkey): A magnetic polarity time scale for the Norian. Earth Planet. Sci. Lett. 117, 443–456.
Gallet, Y., Besse, J., Krystyn, L., Theveniaut, H., Marcoux, J., 1994. Magnetostratigraphy of the Mayerling section (Austria) and Erenkolu Mezarlik (Turkey) section: Improvement of the Carnian (late Triassic) magnetic polarity time scale. Earth Planet. Sci. Lett. 125, 173–191.
Gallet, Y., Besse, J., Krystyn, L., Marcoux, J., 1996. Norian magnetostratigraphy of the Scheiblkogel section Austria: constraint on the origin of the Antalya Nappes, Turkey. Earth Planet. Sci. Lett. 140, 113–122.
Gallet, Y., Besse, J., Krystyn, L., Marcoux, J., Guex, J., Theveniaut, H., 2000. Magnetostratigraphy of the Kavaalani section (southwestern Turkey): consequence for the origin of the Antalya Calcareous nappes (Turkey) and for the Norian (Late Triassic) magnetic polarity timescale. Geophys. Res. Lett. 27, 2033–2036.
Graham, J.W., 1949. The stability and significance of magnetism in sedimentary rocks. J. Geophys. Res. 54, 131–167.
Gullo, M., 1996. Conodont biostratigraphy of uppermost Triassic deep-water calcilutites from Pizzo Mondello (Sicani Mountains): evidence for Rhaetian pelagites in Sicily. Palaeogeogr. Palaeoclimatol. Palaeoecol. 126, 309–323.
Hounslow, M.W., Maher, B.A., Thistlewood, L., Dean, K., 1995. Magnetostratigraphic correlations in two cores from the late Triassic Lunde Formation, Beryl Field, northern North Sea, UK. In: Turner, P., Turner, A., (Eds.), Palaeomagnetic Applications in Hydrocarbon Exploration and Production. Geol. Soc. Lond. Spec. Publ. 98, pp. 163–172.
Huber, P., Lucas, S.G., 1996. Vertebrate biochronology of the Newark Supergroup. Mus. North. Ariz. Bull. 60, 179–186.
Huber, P., Lucas, S.G., Hunt, A.P., 1993. Vertebrate biochronology of the Newark Supergroup, Triassic, eastern North America. In: Lucas, S.G., Morales, M. (Eds.), The Non-Marine Triassic. New Mexico Museum of Natural History and Science, Bulletin 3, pp. 179–186.
Kent, D.V., Olsen, P.E., Witte, W.K., 1995. Late Triassic–earliest Jurassic geomagnetic polarity sequence and paleolatitudes from drill cores in the Newark rift basin, eastern North America. J. Geophys. Res. 100, 14,965–14,998.
Kent, D.V., Olsen, P.E., 1999. Astronomically tuned geomagnetic timescale for the Late Triassic. J. Geophys. Res. 104, 12831–12841.
Kent, D.V., Olsen, P.E., 2000. Implications of astronomical climate cycles to the chronology of the Triassic. Zentralblatt für Geologie und Paläontologie 1, Jahrgang 1998 (11–12), 1463–1473.
Kirschvink, J.L., 1980. The least squares lines and planes analysis of paleomagnetic data. Geophys. J. R. Astron. Soc. 62, 699–718.
Kovács, S., Nagy, G., 1989. A Pilis hegység aviculás és halobiás mészköösszletének kora. MÁFI Évi Jelentése 1987, 95–129.
Kozur, H., 1972. Die Conodontengattung *Metapolygnathus* HAYASHI 1968 und ihr stratigraphischer Wert. Geol. Paläont. Mitt. Innsbruck 2, 1–37.
Kozur, H., 1980. Revision der Conodontenzonierung der Mittel- und Obertrias des tethyalen Faunenreichs. Geol. Paläont. Mitt. Innsbruck 10, 79–172.
Kozur, H., 1989. Significance of events in conodont evolution for the Permian and Triassic stratigraphy. Cour. Forsch.-Inst. Senckenberg 117, 385–408.
Kozur, H., 1989. *Norigondolella n.* gen., eine neue obertriassische Conodontengattung. Paläontol. Z. 64, 125–132.
Kozur, H., 1991. The evolution of the Meliata–Hallstatt ocean and its significance for the early evolution of the Eastern Alps and Western Carpathians. Palaeogeogr. Palaeoclimatol. Palaeoecol. 87, 109–135.
Kozur, H., 1993. Annotated correlation tables of the Germanic Buntsandstein and Keuper. In: Lucas, S.G., Morales, M. (Eds.), The Non-Marine Triassic. New Mexico Museum of Natural History and Science Bulletin 3, pp. 243–248.
Kozur, H., 1996. The position of the Norian–Rhaetian boundary. In: Jost Wiedmann Symposium, Abstracts, Ber. Rep. Geol.-Paläont. Univ. Kiel, 76, pp. 27–35.
Kozur, H., 1997. Pelagic Permian and Triassic of the Western Tethys and its paleogeographic and stratigraphic significance. 48th Berg- und Hüttenmännischer Tag, Kolloquium 1, Stratigraphie, Sedimentation und Beckenentwicklung im Karbon und Perm, Freiberg, pp. 21–25.
Kozur, H.W., 1998. Upper Triassic Punciacea, the connecting link between the Paleozoic to Lower Triassic Kirkbyacea and the Cretaceous to Cenozoic Punciacea. In: Crasquin-Soleau, S., Braccini, E., Lethiers, F. (Eds.), What about Ostracoda! Actes du 3e Congrès Européen des Ostracodologistes, 1996, Bull. Centre Rech. Elf Explor. Prod., Mém. 20, Pau, pp. 257–269.
Kozur, H.W., 1999a. Remarks on the position of the Norian–Rhaetian boundary. Zbl. Geol. Paläont., Teil I, 1998 (7–8), 523–535.
Kozur, H.W., 1999b. The correlation of the Germanic Buntsandstein and Muschelkalk with the Tethyan scale. Zbl. Geol. Paläont., Teil I, 1998 (7–8), 701–725.
Kozur, H.W., 2000. Northern origin of the Antalya and Alanya Nappes (Western Taurus, Turkey) and causes for the end of the Tethyan faunal provincialism during the middle Carnian. Proceedings of the Second Croatian Geological Congress, Zagreb, pp. 275–282.
Kozur, H., Mock, R., 1972a. Neue Conodonten aus der Trias der Slowakei und ihr stratigraphischer Wert. Geol. Paläont. Mitt. Innsbruck 2, 1–20.
Kozur, H., Mock, R., 1972b. Neue Holothurien-Sklerite aus der Trias der Slowakei. Geol. Paläont. Mitt. Innsbruck 2, 1–47.
Kozur, H., Mock, R., 1973a. Die Bedeutung der Trias-Con-

odonten für die Stratigraphie und Tektonik der Trias in Westkarpaten. Geol. Paläont. Mitt. Innsbruck 3, 1–14.

Kozur, H., Mock, R., 1973b. Das Alter der Hauptspaltengeneration in den Hallstatter Kalken des Salzkammergutes (Österreich) und der Slowakei. Geol. Paläont. Mitt. Innsbruck 3, 1–20.

Kozur, H., Mock, R., 1973c. Zum Alter und zur tektonischen Stellung der Meliata-Serie des Slowakischen Karstes. Geol. Zborn. Geol. Carpathica 24, 365–374.

Kozur, H., Mock, R., 1974a. Holothurien-Sklerite aus der Trias der Slowakei und ihre stratigraphische Bedeutung. Geol. Zborn. Geol. Carpathica 25, 115–145.

Kozur, H., Mock, R., 1974b. Zwei neue Conodonten-Arten aus der Trias des Slowakischen Karstes. Časopis Min. Geol. Roč. 19, 135–139.

Kozur, H., Mock, R., 1974c. *Misikella* posthernsteini n. sp., die jüngste Conodontenart der tethyalen Trias. Časopis Min. Geol. Roč. 19, 245–250.

Kozur, H., Mock, R., 1974d. Die Obergrenze der karnischen Dasycladaceen-Kalke in der Lokalität Silická Brezová (Slowakischer Karst). Vest. Ústr. Ústav Geol. 49, 223–225.

Kozur, H., Mock, R., 1991. New Middle Carnian and Rhaetian conodonts from Hungary and the Alps. Stratigraphic importance and tectonic implications for the Buda Mountains and adjacent areas. Jb. Geol. B.-A. 134, 271–297.

Kozur, H., Mock, R., 1996. New paleogeographic and tectonic interpretations in the Slovakian Carpathians and their implications for correlations with the Eastern Alps, Part I. Central Western Carpathians. Mineralia Slovaca 28, 151–174.

Kozur, H., Mock, R., 1997. New paleogeographic and tectonic interpretations in the Slovakian Carpathians and their implications for correlations with the Eastern Alps and other parts of the Western Tethys, Part II. Inner Western Carpathians. Mineralia Slovaca 29, 164–209.

Kozur, H.W., Mock, R., Channell, J.E.T., Aubrecht, R., in press. Carnian–Norian conodont biostratigraphy, taxonomy and magnetostratography at Silická Brezová (Slovakia): implications for Upper Triassic stratigraphy. Hallesches Jahrb. Geowiss., B, Geol. Palaeontol. Min., Beihefte (in press).

Kozur, H., Mostler, H., 1972. Die Bedeutung der Conodonten für stratigraphische und palaogeographische Untersuchungen in der Trias. Mitt. Ges. Geol. Bergbaustud. Innsbruck 21, 777–810.

Kruczyk, J., Kadzialko-Hofmokl, M., Tunyi, I., Pagac, P., Mello, J., 1998. Paleomagnetic study of Triassic sediments from the Silica nappe in the Slovak Karst, a new approach. Geologica Carpathica 49, 33–43.

Krystyn, L., 1980. Stratigraphy of the Hallstatt region. Abh. Geol. B.-A., 35, Wien, pp. 69–98.

Krystyn, L., 2002. In search of a Tethyan Carnian–Norian boundary GSSP. In: IUGS Subcommission on Triassic Stratigraphy. STS/IGCP 467 Field Meeting, Veszprém, Hungary, 5-8 September, 2002, Budapest, pp. 49–50.

Lowrie, W., 1990. Identification of ferromagnetic minerals in a rock by coercivity and unblocking temperature properties. Geophys. Res. Lett. 17, 159–162.

Lucas, S.G., 1998. Global Triassic tetrapod biostratigraphy and biochronology. Palaeogeogr. Palaeoclimatol. Palaeoecol. 143, 347–384.

Lucas, S.G., Heckert, A.B., 2001. The aetosaur *Stagonolepis* from the Upper Triassic of Brazil and its biochronological significance. N. Jb. Geol. Paläontol. Mh. 20001, 719–732.

Marcoux, J., Ricou, L.E., Brun, J.-P., 1989. Shear sense criteria in the Antalya and Alanya thrust system (southwestern Turkey): evidence for a southward emplacement. Tectonophysics 161, 89–91.

Marton, E., Marton, P., Less, G., 1988. Palaeomagnetic evidence of tectonic rotations in the southern margin of the Inner West Carpathians. Phys. Earth Planet. Inter. 52, 256–266.

Marton, P., Rozloznik, L., Sasvari, T., 1991. Implications of a palaeomagnetic study of the Silica nappe, Slovakia. Geophys. J. Int. 107, 67–75.

McFadden, P.L., 1990. A new fold test for palaeomagnetic studies. Geophys. J. Int. 103, 163–169.

Mišík, M., Borza, K., 1976. Obere Trias be Silická Brezová (Westkarpaten). Acta Geol. et Geograph. Univ. Comeniane, Bratislava 30, 5–49.

Mock, R., 1980. Field Trip D 'Triassic of the West Carpathians, in Second European conodont symposium' ECOS II. Abhandl. Geol. Bundesanst. 35, 129–144.

Mundil, R., Brack, P., Meier, M., Rieber, H., Oberli, F., 1996. High resolution U–Pb dating of Middle Triassic volcaniclastics: time-scale calibration and verification of tuning parameters for carbonate sedimentation. Earth Planet. Sci. Lett. 141, 137–151.

Muttoni, G., Channell, J.E.T., Nicora, A., Rettori, R., 1994. Magnetostratigraphy and biostratigraphy of an Anisian–Ladinian (Middle Triassic) boundary sections from Hydra (Greece). Palaeogeogr. Palaeoclimatol. Palaeoecol. 111, 249–262.

Muttoni, G., Kent, D.V., Meco, S., Nicora, A., Gaetani, M., Balini, M., Germani, D., Rettori, R., 1996. Magneto–biostratigraphy of the Spathian to Anisian (Lower to Middle Triassic) Kcira section, Albania. Geophys. J. Int. 127, 503–514.

Muttoni, G., Kent, D.V., Brack, P., Nicora, A., Balini, M., 1997. Middle Triassic magneto–biostratigraphy from the Dolomites and Greece. Earth Planet. Sci. Lett. 146, 107–120.

Muttoni, G., Kent, D.V., Meco, S., Balini, M., Nicora, A., Rettori, R., Gaetani, M., Krystyn, L., 1998. Towards a better definition of the Middle Triassic magnetostratigraphy and biostratigraphy in the Tethyan realm. Earth Planet. Sci. Lett. 164, 285–302.

Muttoni, G., Kent, D.V., Di Stefano, P., Gullo, M., Nicora, A., Tait, J., Lowrie, W., 2001. Magnetostratigraphy and biostratigraphy of the Carnian/Norian boundary interval from Pizzo Mondello section (Sicani Mountains, Sicily). Palaeogeogr. Palaeoclimatol. Palaeoecol. 166, 383–399.

Nowlan, G.S., Barnes, C.R., 1987. Application of conodont alteration indices to regional and economic geology. In: Austin, R.L. (Ed.), Conodonts Investigative Techniques and Applications. Ellis Horwood, pp. 188–202.

Olsen, P.E., Kent, D.V., 1996. Milankovitch climate forcing in the tropics of Pangaea during the Late Triassic. Palaeogeogr. Palaeoclimatol. Palaeoecol. 122, 1–26.

Olsen, P.E., Kent, D.V., 1999. Long-period Milankovitch cycles from the Late Triassic and Early Jurassic of eastern North America and their implications for the calibration of the Early Mesozoic time-scale and long-term behavior of the planets. Philos. Trans. R. Soc. Lond. A 357, 1761–1786.

Opdyke, N.D., Channell, J.E.T., 1996. Magnetic Stratigraphy. Academic Press, 346 pp.

Orchard, M.J., 1991a. Upper Triassic conodont biochronology and new index species from the Canadian Cordillera. Geol. Surv. Can. Bull. 417, 299–335.

Orchard, M.J., 1991b. Late Triassic conodont biochronology and biostratigraphy of the Kunga Group, Queen Charlotte Islands, British Columbia. In: Evolution and Hydrocarbon Potential of the Queen Charlotte Basin, British Columbia. Geol. Surv. Can. Pap. 90-10, pp. 173–193.

Orchard, M.J., Carter, E.S., Tozer, E.T., 2000. Fossil data and their bearing on defining a Carnian–Norian (Upper Triassic) boundary in western Canada. Albertiana 24, 43–50.

Orchard, M.J., Tozer, E.T., 1997. Triassic conodont biochronology, its calibration with the ammonoid standard, and a biostratigraphic summary for the western Canada sedimentary basin. Bull. Can. Pet. Geol. 45, 675–692.

Pálfy, J., Smith, P.L., Mortensen, J.K., 2000. A U–Pb and $^{40}Ar/^{39}Ar$ time scale for the Jurassic. Can. J. Earth Sci. 37, 923–944.

Pálfy, J., Smith, P.L., Mortensen, J.K., 2002. Dating the end-Triassic and Early Jurassic mass extinctions, correlative age igneous provinces, and isotopic events. In: Koeberl, C., MacLeod, K. (Eds.), Catastrophic Events and Mass Extinctions: Impacts and Beyond. Geol. Soc. Am. Spec. Pap. 356 (in press).

Steiner, M.B., Lucas, S.G., 2000. Paleomagnetism of the Late Triassic Petrified Forest Formation, Chinle Group, western United states: further evidence of 'large' rotation of the Colorado Plateau. Tectonics 105, 25,791–25,808.

Tunyi, I., Vass, D., Elecko, M., 1999. Tectonic interpretation of palaeomagnetic measurements in area of Drienovec village (Eastern Slovakia). Mineralia Slovaca 31, 61–68.

Watson, G.S., 1956. A test for randomness of directions. Mon. Not. R. Astron. Soc. Geophys. Suppl. 7, 289–300.